Thesis for the Degree of Master of Engineering

The Cutting Performance of TiSiCN Hard Coating Deposited by PEMS (Plasma-Enhanced Magnetron Sputtering)

by

LIU ZHENHUA

Department of Mechanical Engineering

The Graduate School

Pukyong National University

February 2009

The Cutting Performance of TiSiCN Hard Coating Deposited by PEMS (Plasma-Enhanced Magnetron Sputtering)

Advisor: Prof. Kyu-Yong Lee

by

LIU ZHENHUA

A thesis submitted in partial fulfillment of the requirements
For the degree of
Master of Engineering

in Department of Mechanical Engineering, The Graduate School, Pukyong National University

February 2009

The Cutting Performance of TiSiCN Hard Coating Deposited by PEMS (Plasma-Enhanced Magnetron Sputtering)

A dissertation

By

LIU ZHENHUA

Approved by:

(Chairman) Prof. Yoon Moon Chul

(Member) Prof. Kim Seon Jin

(Member) Prof. Kyu Yong Lee

February 25, 2009

Contents

The Cutting Performance of TiSiCN Hard Coating Deposited by PEMS (Plasma-Enhanced Magnetron Sputtering)

LIU ZHENHUA

Department of Mechanical Design Engineering, The Graduate School,

Pukyong National University

Abstract

In this current investigation, we applied a developed physical vapour deposition process named Plasma-Enhanced Magnetron Sputtering(PEMS) to coat TiSiCN thin film on WC-Co cutting inserts, column structure is eliminated by applying heavy ion bombardment, high deposition rate up to 7um/h was achieved and large thickness was measured around 5um, three samples were used to study the deposition technique and the high speed dry cutting properties on the carbon steel. Scratch test was used to investigate adhesion of the TiSiCN coatings which indicated critical load can be over 55 N, surface morphology and microstructure of the TiSiCN coatings were revealed by SEM(Scanning Electron Microscope), AFM(Atomic Force Microscope), XRD(X-ray diffraction Microscope).

Cutting experiment was carried out through face milling medium carbon steel in the CNC center under dry condition, cutting resistant force can be significantly reduced by 80% compared with the raw insert, the chip formation, BUE (build-up edge) and adhesion wear were investigated, in the end, the Vickers Indentation fracture toughness was revealed by different calculations. According to our first attempt, this super hard coating TiSiCN can be applied as a protection layer on the WC-Co cutting tools in high speed cutting under dry condition

I. Introduction

1. Dry Enabled HSM

There are several definitions of HSM(High Speed Machine), but the most common is based upon the rpm of the machine tool spindle. Operating above that spindle speed requires special attention to details such as spindle balance, machine setup, coolant application, tool paths and wear patterns [1]. The key concept is the need to manipulate speed, feed and DOC to increase metal removal rates while lowering cutting forces. In a word, HSM is geared toward high production, it offers several advantages over conventional machining such as:

1) Great reduction in machining time
2) Reduces overheating of the workpieces due to faster feeds
3) Low surface roughness
4) Less residual stress

In many cases, HSM enables dry machining as well, as it eliminates coolant use, reduces cutting costs and providing a healthier working environment [2]. However, even with the sharpest tools, high temperatures build up quickly and must be diverted away from the tool, so, dry machining usually needs for a soft, non-stick coating and a suitable tool geometries to prevent overheating, work hardening and serious geometric and dimensional flaws.

In the machining, served as a base material, sintered hexagonal crystal structured WC-Co is widely used since their development in the 1920s due to:

1) Tungsten carbide has very high strength for a material so hard and rigid. Compressive strength is higher than virtually all melted and cast or forged metals and alloys.
2) Tungsten carbide compositions range from two to three times as rigid as steel and four to six times as rigid as cast iron and brass.

3) For such a hard material with very high rigidity, the impact resistance is high.
4) Tungsten-base carbides perform well up to about 600℃ in oxidizing atmospheres and to 800°C in non-oxidizing atmospheres
5) Tungsten carbide compositions exhibit low dry coefficient of friction values as compared to steels.
6) Tungsten carbide compositions have exceptional resistance to galling and welding at the surface.
7) Specific grades are available with corrosion resistance approaching that of noble metals. Conventional grades have sufficient resistance to corrosion-wear conditions for many applications.
8) Wear resistance of tungsten carbide is better than that of wear-resistance tool steels.

However, in the HSM, the WC-Co is no longer suitable candidate to be as a cutting tools since in the HSM, especially under dry cutting, machining conditions may submit the contact area of tools surface to higher temperature, where the mechanical properties of cemented tungsten carbide-cobalt are strongly degraded mainly due to the severe oxidation, severe adhesion problem and build-up edge may occur.

Due to such several reasons listed above, the coating has been applied on the cutting tools since the last century, and it is still remained large potential market so far, nowadays more and more coating companies are established in German, USA, UK, Japan, China and spread all over the world, most of the companies serve at applying coating on the cutting tools and also developing new and more suitable and special coating for a certain goal, they also declaimed that “everything is coated”. Up to now, several coatings are applied in the material-removing process such as TiN, TiCN, TiAlN, DLC [3] and so on, coatings increase tool hardness, toughness, and heat resistance, permitting long tool runs at aggressive speeds and feeds. In addition, coatings can reduce machining friction and heat buildup, resulting in less machine wear, tool crater,

and flute packing. Another bonus is that coatings have no chemical affinity to workpiece materials, so they resist edge buildup and galling. The coatings developed so far can be classified as:

1) Single layer and multilayer based on the architecture
2) Ternary, quaternary, or pentnary systems based on the element that coatings consist of
3) Ceramic, polymer, metal…coating based on the coating material's chemical composition
4) Optical and tribological coating based on the application
5) PVD and CVD coating based on the process that coating was deposited

Usually, multilayered structure is used as a protective coating to increase its adhesion to the substrate. Guhring [4] used a unique cathodic arc process to introduce its multilayer Firex hard coating in cooperation with Platit of Switzerland. This coating combines layers of titanium nitride(TiN), titanium aluminum nitride(TiAlN), and titanium carbon nitride(TiCN) and features a hardness of over 90 Rc. Its maximum operating temperature is 800 °C.

2. Plasma and Surface Modification

So, how to deposit coatings on the cutting tool? The deposition process is always carried on in the plasma-generated vacuum chamber, so, the plasma technique in the deposition and surface modification mechanism should be seriously considered.

2.1 Plasma

Except solid, liquid and gas, plasma exists as the fourth of matter in the world which was first found by Sir William Crookes [5] in 1879 (he called it "radiant matter"), he defined plasma as positive ions and negative electrons in a sea of

neutral atoms. Ion-electron pairs are continuously created by ionization and destroyed by recombination. Since these processes are always existing pairwise , the space occupied remains charge neutral. Since three set of particles exist in the ions, electrons, neutrals varying by mass and temperature.

If we suspend a small electrically isolated substrate into the plasma, initially, it will be struck by electrons and ions with charge fluxes,

$$j_e = \frac{en_e\bar{c}_e}{4}, \qquad j_i = \frac{en_i\bar{c}_i}{4} \quad \cdots\cdots\cdots\cdots\cdots\cdots\cdots \text{(Eq 2.1.1)}$$

Since $\bar{c}_e$ is much larger than $\bar{c}_i$, then the substrate immediately starts to build a negative charge and hence negative charge potential with respect to the plasma, immediately the quasi-random motion of ions and electrons in the region of our object, are distributed, since the substrate charged negatively, electrons are repelled and ions are attracted, thus the electrons fluxes decrease, but the object continued to charge negatively until the electron flux is reduced by repulsion just enough to balance the ion flux, we shall show shortly("Debye Shielding") that the plasma is virtually electric field free, except around perturbations such as above, and so is equipotential, similarly, with the isolated substrate, in the case of a plasma container having insulating walls, these walls also require zero steady state ne flux, so that wall potential and float potential are related terms, since Vf is such as to repel electrons, then Vf<Vp, in the absence if a reference, only the potential difference Vp-Vf is meaningful. Because of the charging of substrate, it is as though a potential energy hill develops in front of the substrate, but uphill for the electrons, so that only those electrons with enough energy initial kinetic energy make it to the top, i.e. the substrate [6].

In DC plasma, although the electrons and ions are in equilibrium as a whole, this is the only average result of the many detailed interactions, if a plasma is perturbed from neutrality for any reasons, then there will be large restoring forces

striving to reestablish charge neutrality, the electrons are first to respond to the restoring force since the low mass. The plasma state is rich in wave phenomena when the degree of ionization is large enough to make long-range forces important, particularly when a magnetic field is present. Departure from charge neutrality capable of generation waves can occur in the form of charge bunching and separation over distances of the order of the Debye length. Let's consider the case of a plasma in a uniform electric field, as illustrated in the Fig. 1, there is an $\vec{E}\times\vec{B}$ drift perpendicular to the both electric field and magnetic field, but in the absence of collisions, simple theory predicts no transport across the magnetic field in the direction of electric field. If charge bunching occurs, the perpendicular produces an electric field $\overrightarrow{E_p}$ that can result in $\vec{E}\times\vec{B}$ drift across the magnetic field in the direction of $\vec{E}$. This anomalous collisionless transport across the magnetic field is believed to be an important mechanism in Penning discharge as well as in some magnetron sputtering discharge.

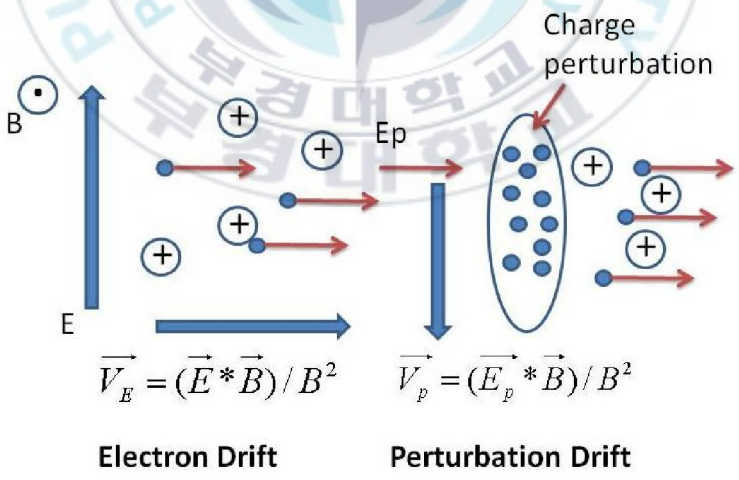

Fig. 1 Schematic representation of a plasma instability resulting in electron transport across a magnetic field

2.2DC Glow Discharge

As our work involved in, only DC glow discharge is considered. Glow discharge owns its name to the fact that plasma is luminous. The glow can be produced by applying a potential difference between two electrodes in a gas. The potential drops rapidly close to the cathode, varying slowly in the plasma, and change again close to the anode. The electric fields in the system are restricted to sheaths at each of the electrodes. The sheath fields are such as to repel electrons trying to reach either electrode. Electrons originating at the cathode will be accelerated, collide, transfer energy, leave by diffusion and recombination, slow by the anode and get transferred into the outside circuit. The luminous glow is produced because the electrons have enough energy to generate visible light by excitation collisions. Since there is a continuous loss of electrons, there must be an equal degree of ionization going on to maintain the steady state [7]. The energy is being continuously transferred out of the discharge and hence the energy balance must be satisfied also. Simplistically, the electrons absorb energy from the field, accelerate, ionize some atoms, and the process becomes continuous. Additional electrons are produced by secondary emission from the cathode. These are very important to maintaining a sustainable discharge. Three basic regions are described below in Fig. 2, the cathode region, the glow regions, and the anode region [8].

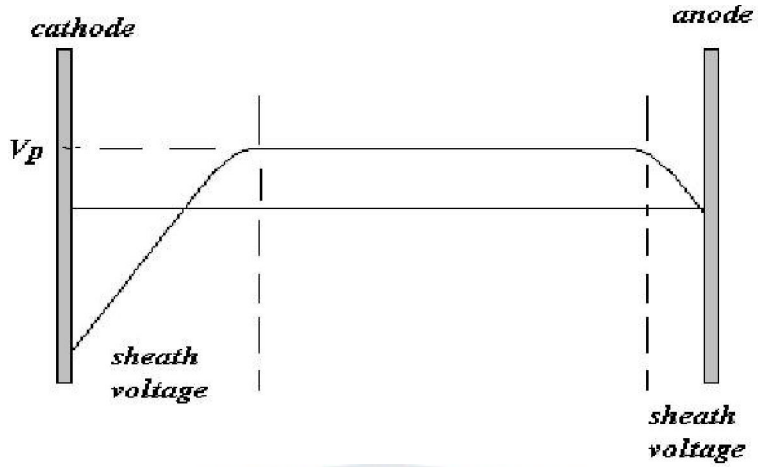

Fig. 2 Voltage distribution in a DC glow discharge

1) The cathode region

The type of dc discharge in glow discharge is named as an abnormal glow discharge, at lower applied voltage and consequent lower current. The cathode plays an important part in dc sputtering system because the sputtering target actually becomes the cathode of the sputtering discharge, the cathode is also the source of secondary electrons, as we have seen, and these secondary electrons have a significantly role both in maintaining the discharge and in influencing the growth of sputtered films. The ionization in the sheath is a very important factor in cathode region as shown in the Fig. 3.

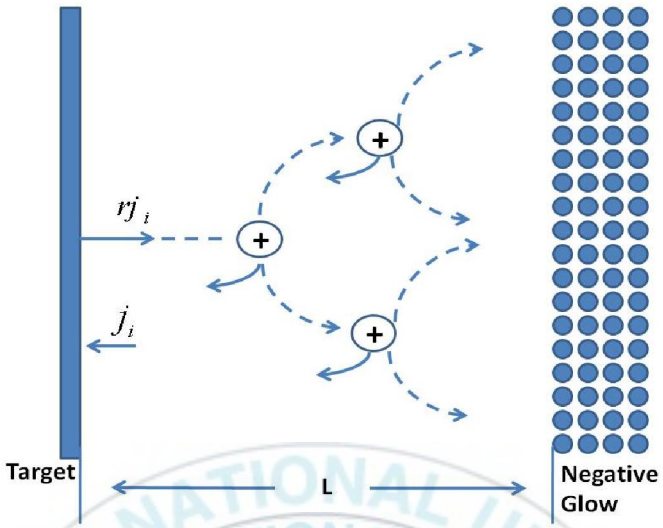

Fig. 3 Ion pare production in the dark space

Ionization is caused by secondary electrons from the target as they are accelerated across the dark space. This is can be modeled by considering the amount of ionization caused by a flux $N_e(x)$ electrons passing through a thin slab of thickness Δx located x from the cathode.

$$N_e(x) = N_e(o)\exp nqx \quad \cdots\cdots\cdots\cdots\cdots\cdots\cdots \text{(Eq 2.2.1)}$$

So, each electron that leaves the target is multiplied by exp nqL by the time it reaches the edge of dark space, the electron field in this region is strong enough that the major part of the electron travel will be straight across the dark space along the field lines.

While the charge exchange is another important factor when an ion arriving the interface between the glow and a sheath, it has a kinetic energy that is negligible compared with most sheath. In the absence of collision, the ion

would accelerate across the sheath, losing potential energy as it does so, and would hit the electrode with an energy equivalent to the sheath voltage.

- The effect of the gas pressure on the energy distribution is small, if the discharge voltage is held constant, this is a result of the pressure- dark space thickness product being fairly constant for a dc discharge, so that the average number of collisions per ion in traversing this distance is reasonably constant.
- Increasing the target voltage causes the dark space to decrease in thickness, so that a relatively larger proportion of high energy ions will reach the cathodes.
- Reduction of the collision cross-section also causes a larger proportion of high energy ions.

Here, the structure of cathode is list below in the Fig. 4, this sheath maybe as much as a few centimeter thickness, the final sheath model has three regions:

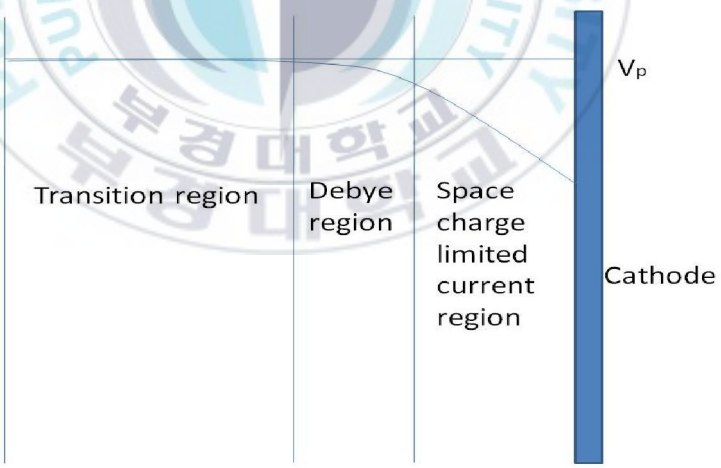

Fig. 4 Regions of a cathode sheath

Region one: a quasi-neutral “pre-sheath” in which ions are accelerated to satisfy the Bohme criterion.

Regions two: a region of extent of a few Debye length in which the electron density rapidly becomes negligible.

Region three: a region of space charge limited current flow, which would be of zero electron density in the absence of secondary electron emission from the target, and in practice is not so different because of the rapid acceleration of the electrons.

2) The anode region

In anode region, the probable main effect is the polarity, which is such as to accelerate secondary electrons from the anode back into the glow, and also to accelerate ions from the glow onto the anode and onto any substrate there. Although the sheath is too thin, to be a likely source of ionization, the accelerated secondary electrons act as both an electron source and an energy source to the glow. The sheath has to rely on the glow as an ion source. Since there appears to be rather little ionization in the cathode sheath and even less in the anode sheath, the ion fluxes at each electrode are of similar magnitude.

3) The glow region

Although the glow is an ionized gas of approximate charge neutrality, it certainly is not uniform isotropic plasma. The main reason for this is the beam of fast electrons entering the glow region from the cathode sheath, these penetrate into and through the sheath and make it very anisotropic. Three groups of electrons in glow are:

- Primary electron which enter from the cathode sheath with high energy, which retain a practically all the momentum acquired by acceleration across the cathode sheath, and hence are directional.
- Secondary electrons of considerably lower energy, these are the product electrons of ionizing collisions of primaries which have lost much of their energy.

- Ultimate electrons which have becomes thermalized to the plasma temperature, these ultimate electrons have the highest density.

In the glow region, the fast electrons, ions and thermal electrons are the causes to ionize.

2.3 Surface Modification Technique

For the past several decades, thanks to the development of surface modification technique, coating was applied on the dry HSM under dry condition to serve as a self-lubricant, wear-protection, friction-reduction layer. The surface modification process can be classified as sub-plantation, implantation, and coating as explained below, according to the particle energies accelerated by the sources. Here, coating is more available because the coatings do not change the properties of the bulk material. In surface modification technique, the ionized particles injected or made reacted with the material surface mainly may result in:

(1) The ion may be reflected, probably being neutralized in the process. This reflection is the basis of an analytical technique known as Ion Scattering Spectroscope.
(2) The impact ion of the ion may help eject an electron, usually referred to as a secondary electron.
(3) The ion may become buried in the target called ion implantation.
(4) The ion impact may also be responsible for some structural rearrangements in the target material. “Rearrangement” may vary from simple vacancies(missing atoms) and interstitials(atoms out of position) to more gross lattice defects such as changes of architecture in alloy or compound targets, or to changes in electrical charge levels and distributions.
(5) The ion impact may set up a series of collisions between atoms of the target, possibly leading to the ejection of one of these atoms. This ejection process in known as sputtering. As indicated in the Fig. 5.

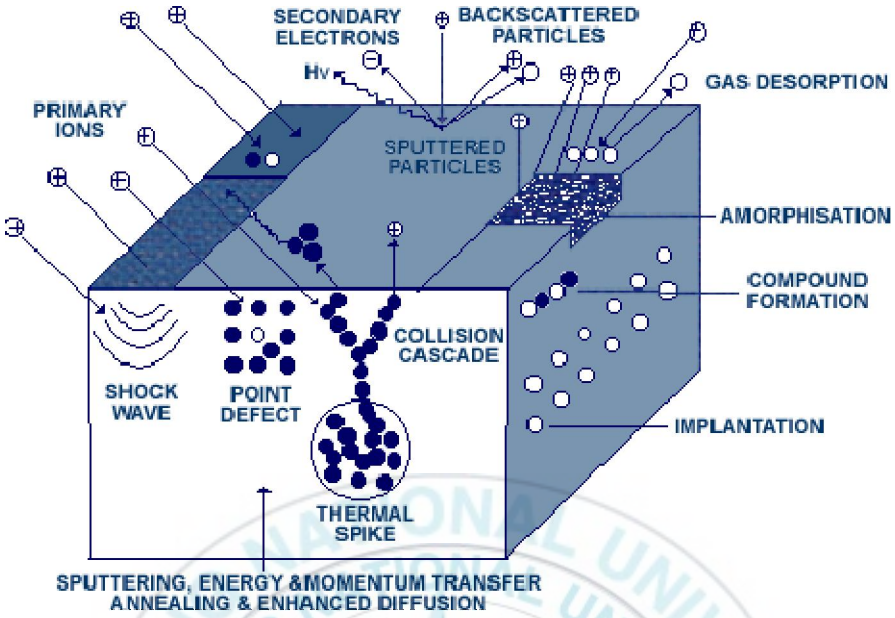

Fig. 5 The schematic of Ion bombardment to surface

The main coating methods can be classified as PVD and CVD depending on the process that the particles were coated on the substrate. CVD process deposits thin film on insert through various chemical reactions, most cutting tools were deposited by CVD until development of PVD, mainly sputtering and evaporation. PVD is becoming increasing favorable over CVD mainly because of the low temperature, in CVD deposition, high temperature causes soften and deformation to many cutting tool substrate, especially HSS, another advantage of PVD deposition is it can deposit thinner film so that it is more easier to obtain multilayered coating through PVD, which was found to reduce wear considerably, it is not possible to point to the best way of preparing a thin film, the methods used must depend on the type of film required, the limitation present on choice of the substrate, and quit often in the case of multiple deposition, the general compatibility of the various processes to be used.

3. Hard Coating

Maybe the most familiar coating is "self-cleaning coating" which is a kind of PVD optical coatings, the coated windows apparently need less maintenance and are easier to clean. The chemical composition of this coating is titanium dioxide, TiO_2, which has photo catalytic and hydrophilic properties.

However, up to now, hard coatings are hindered due to the increasing need of critical factors such as wear, friction coefficient, hardness, toughness, thermally and chemically stability in the dry high speed cutting. For general purposes in increasing the mechanical and enlarging the application of the hard coatings, it is tremendously important to examine to history of developing, and the general application of hard coatings in other areas. The main application and properties characteristic method are often not only give new idea to the new developed coating but also a very good experience to the developing of new hard coating and new applications. Generally, TiN or TiN-based nanocrystalline film and DLC are the most used in the industry application so far.

1) Titanium nitride (TiN) is a hard ceramic (~85 Rockwell C Hardness or ~2500 Vickers Hardness or 24.5 Gpa) [9] coating, often used on titanium alloy, steel, carbide, and aluminum components to improve the substrate's surface properties. TiN has excellent infrared reflectivity properties, reflecting in a spectrum similar to elemental gold. Depending on the substrate material and surface finish, TiN will have a coefficient of friction ranging from 0.4 to 0.9 versus itself unlubricated, it oxidizes at 600°C at normal atmosphere[10~12].
2) Diamond-like carbon (DLC) is a metastable form of amorphous carbon containing a significant fraction of sp3 bonds[13], it can have a high mechanical hardness, chemical inertness, optical transparency, and it is a wide band gap semiconductor. DLC films have widespread applications as protective coatings in areas such as optical windows, magnetic storage disks, car parts, biomedical coatings and as micro-electromechanical devices (MEMs)[14]. DLC has some extreme properties similar to diamond, such as the hardness, elastic modulus and chemical inertness, but these are achieved in an isotropic disordered thin film with no grain boundaries.
3) TiSiCN, as the hard coating developed recently. Since DLC hard coating usually applied for cutting the non-ferrous material and tribology area, it is too thin(less than 1 um), and strong adhesion to the ferrous workpiece material, DLC was hindered for larger area. People went to the TiN based ceramic

material, as developed by several ternary coating such as TiCN, TiAlN, coatings are developed in the direction of high hardness, high wear resistance, high toughness at high stableness at high temperature. Among the coatings latest developed, TiSiN nanocomposite coating have received particular attention because of its much high hardness(40-105Gpa), better thermal stability(up to 1000°C) and higher elastic recovery(up to 80%) as compared with TiN coatings [15~17], but unfortunately, the friction coefficient of TiSiN coating is generally high (0.5-0.8 at both room and elevate temperature) [18], while in the DLC thin film, the transfer film which is graphite carbon phase was formed to be a lubricant layer, the superlow friction coefficient was reported by several researchers. So, by applying C in the TiSiN nanocomposite, a quaternary nanocrystalline structured thin film was conducted.

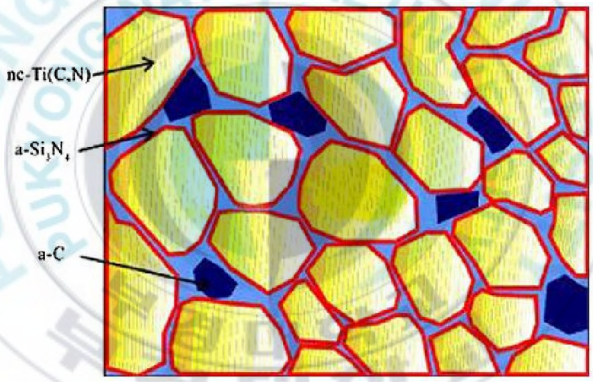

Fig. 6 The typical structure of TiSiCN

Since the typical structure shown as Fig. 6 was reported by number of researchers which consist of nanocrystalline structure Ti(C,N), embedded in the amorphous structure Si_3N_4 and amorphous carbon [18]. However, TiSiCN thin film was reported to be coated only in the CVD way by now, typical structure of TiSiCN was nearly developed, very few papers were published at this area, researchers reported that the TiSiCN has great potential to be applied on the cutting process, but rare experiments were carried on, applications and properties of TiSiCN are far from completely known. Since there are several pioneers on the TiSiCN coating who are working on the characteristics of the coating, the erosion

properties, thermal and chemical properties, mechanical properties such as hardness, elastic modulus, and tribology properties such as friction , it is naturally for us to apply such a coating to HSM under dry condition, in this work, we are attempted to apply TiSiCN thin film on WC-Co insert the cutting carbon steel workpiece, adhesion wear, cutting force, roughness indentation fracture are the main factors we concerned.

Ⅱ . Experiment

1. PEMS

Three triangle cutting inserts WC-Co were used to study this technology which were named PK21, PK22, PK23. The samples were polished using 1 μm diamond paste to a surface roughness of 5 nm Ra. They were cleaned with acetone and methanol before entering the vacuum chamber for processing.

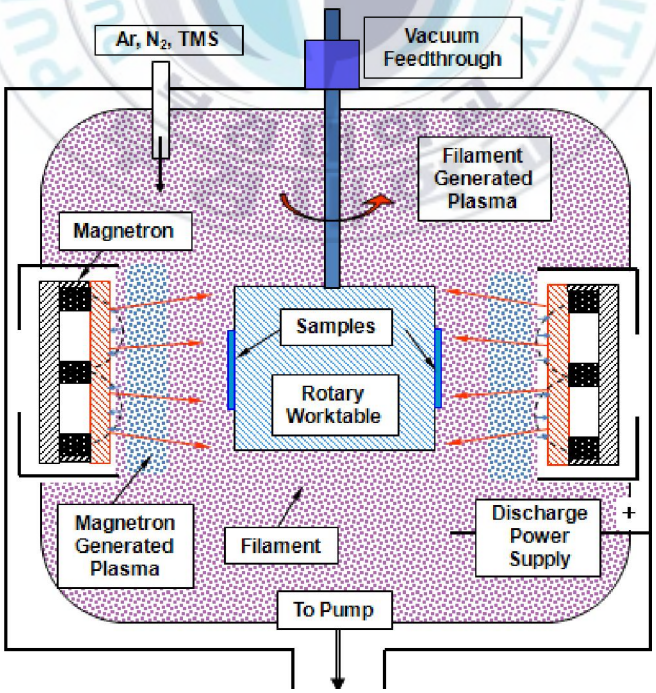

Fig. 7 Schematics of PEMS

Shown in Fig. 7 is a schematic of the DC-PEMS system. As can be seen, the PEMS technology utilizes an electron source (a heated filament) and a discharge power supply to generate plasma. This electron-source generated plasma is independent of the magnetron-generated plasma. There are a number of advantages of this technique. First, during the substrate sputter-cleaning, the magnetrons is not operated, while the electron-source generated plasma alone is sufficient to clean the substrate, in the cathode region, the happening of ion bombardment is rarely less which is insufficiently to cause large number of target atom to sputtered from the target, in this case, it is much better to prevent contaminations at the substrate, while at the anode region, the energy for sputtering clean is less corresponding to the low plasma density, the contaminations in the surface of workpiece is successfully removed due to the low energy sputtering, while the sputtering clean is ensured in this way, while in conventional sputtering clean, they contaminations usually still existed while sputtering happened at the cathode region. Second, during the film deposition, the ion bombardment from the electron-source generated plasma is very intense and the current density at the sample surfaces can be 25 times higher than that with the magnetron-generated plasma alone, as discussed before, the deposition rate is much more effected by the current rather than voltage. Consequently, a high ion-to-atom ratio can be achieved.

But how to obtain element Silicon in the coating is really not a easy task, it is difficult to use two separate targets of Ti and Si to obtain a uniform coating across a large area. In addition, the sputtering rate controlling for Si is not an easy task especially in the N_2 environment. In several CVD deposition process[18~22], the element of silicon was obtained use the gas of SiH_4 or $SiCl_4$, while actually they are not good candidates since they are

pyrophoric gases and requires special equipment for the gas handling and safety training for the operators. Trimethylsilane(TMS) is flammable but not pyrophoric and can be handled in a similar way as many other flammable gases and should not cause severe corrosion to the vacuum chamber and pumps. In this PEMS, DC biased glow discharge was applied at a chamber with two sides of magnetrons, high deposition coefficient was obtained while the specimens were placed in the rotated shaft to be deposited in a vacuum as indicated in the Fig. 8 list below.

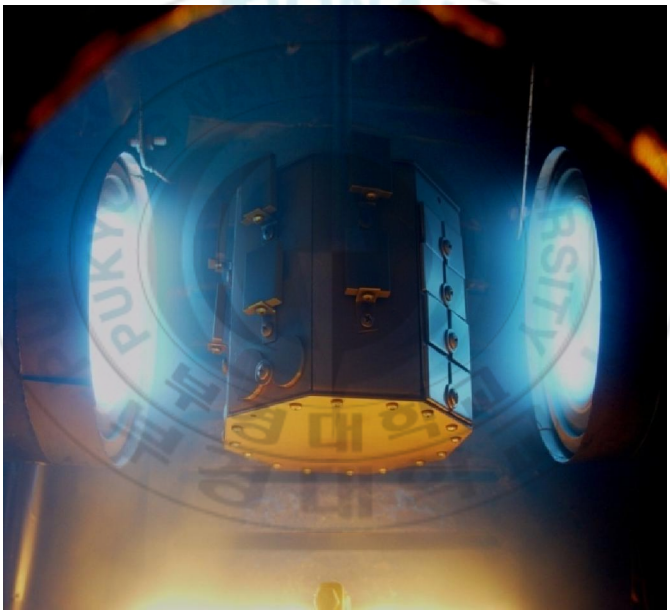

Fig. 8 Depositing in the PEMS(Image)

2. Coating characteristic and cutting test

Coating thickness was measured using SEM cross-section method, three samples were used to study the deposition technique and the high speed dry cutting properties on the carbon steel.

Scratch test was used to investigate adhesion of the TiSiCN coatings schematically showed in Fig. 9, in the scratch process, the coating sample is fixed lying under the diamond tip which is linked with a strain-gauge sensor. Along with the moving stage, the load increased, typically up to 100N(judged by the coating properties), the diamond tip gradually causes damage along with the increasing load, and the sensor acquired the responding signals. The normal load and friction load are recorded and then COF can be calculated.

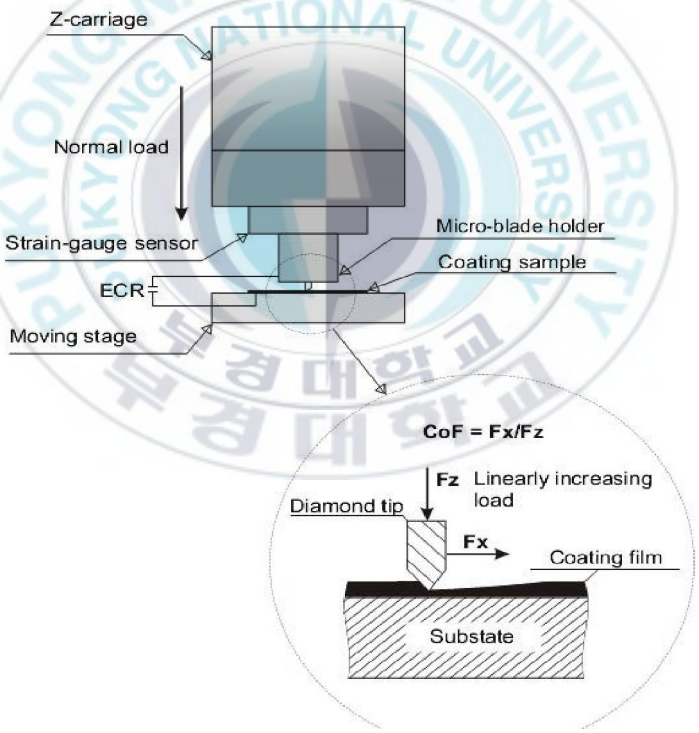

Fig. 9 Schematics of Scratch tester

Then, surface morphology and microstructure of the TiSiCN coatings were revealed by SEM(Scanning Electron Microscope), AFM(Atomic Force Microscope), XRD(X-ray diffraction Microscope) schematically showed in the Fig. 10. When X-rays interact with a crystalline substance, one gets a diffraction pattern. X-rays primarily interact with electrons in atoms. When x-ray photons collide with electrons, some photons from the incident beam will be deflected away from the direction where they original travel. The peaks in a x-ray diffraction pattern are directly related to the atomic distances. See an incident x-ray beam interacting with the atoms arranged in a periodic manner as shown in 2 dimensions in the following Fig. 10.

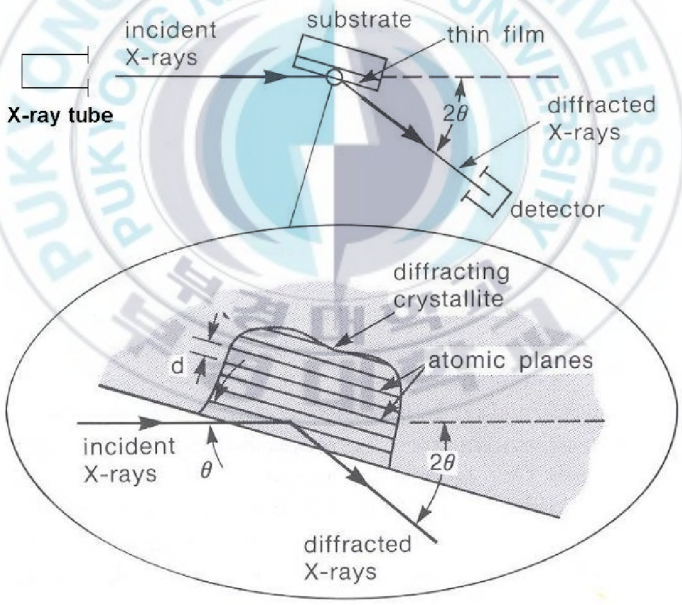

Fig. 10 The schematic of XRD diagram

Surface toughness of coated specimens was measured using surface roughness tester and Vickers indentation hardness was obtained through Vickers Hardness

Tester(SJ-301, Mitutoyo Corporation). Cutting experiment was carried out through face milling medium carbon steel in the CNC center under dry condition, cutting resistant force and surface roughness of workpiece were measured, the chip formation, BUE (build-up edge) and adhesion wear were investigated. AISI 1040 median carbon steel's data sheet is list below as Tab. 1.

Tab. 1 Composition of the workpiece material

Composition	C	Mn	P	S
Element Weight%	0.37-0.44	0.60-0.90	0.04(Max)	0.05(Max)

The cutting resistance force test was prepared in a cutting condition that: RPM is 3000rpm, cutting depth is set as 1 mm, the feed is set as 150mm/min, humidity is not measured but assumed as 50%.

Fig. 11 USB6122 DAQ card, dynamometer and amplifier

The median carbon steel workpiece was fixed in a Computer Numerical Control (CNC) Milling Machine, gradually cutting data was acquired by a NI(National Instrument) DAQ card(USB-6211) linked with a dynamometer sensor, KISTEL 9272B and a computer installed with a Labview7.1. Some equipments are listed in the Fig. 11, and the main steps are listed below as Fig. 12 too.

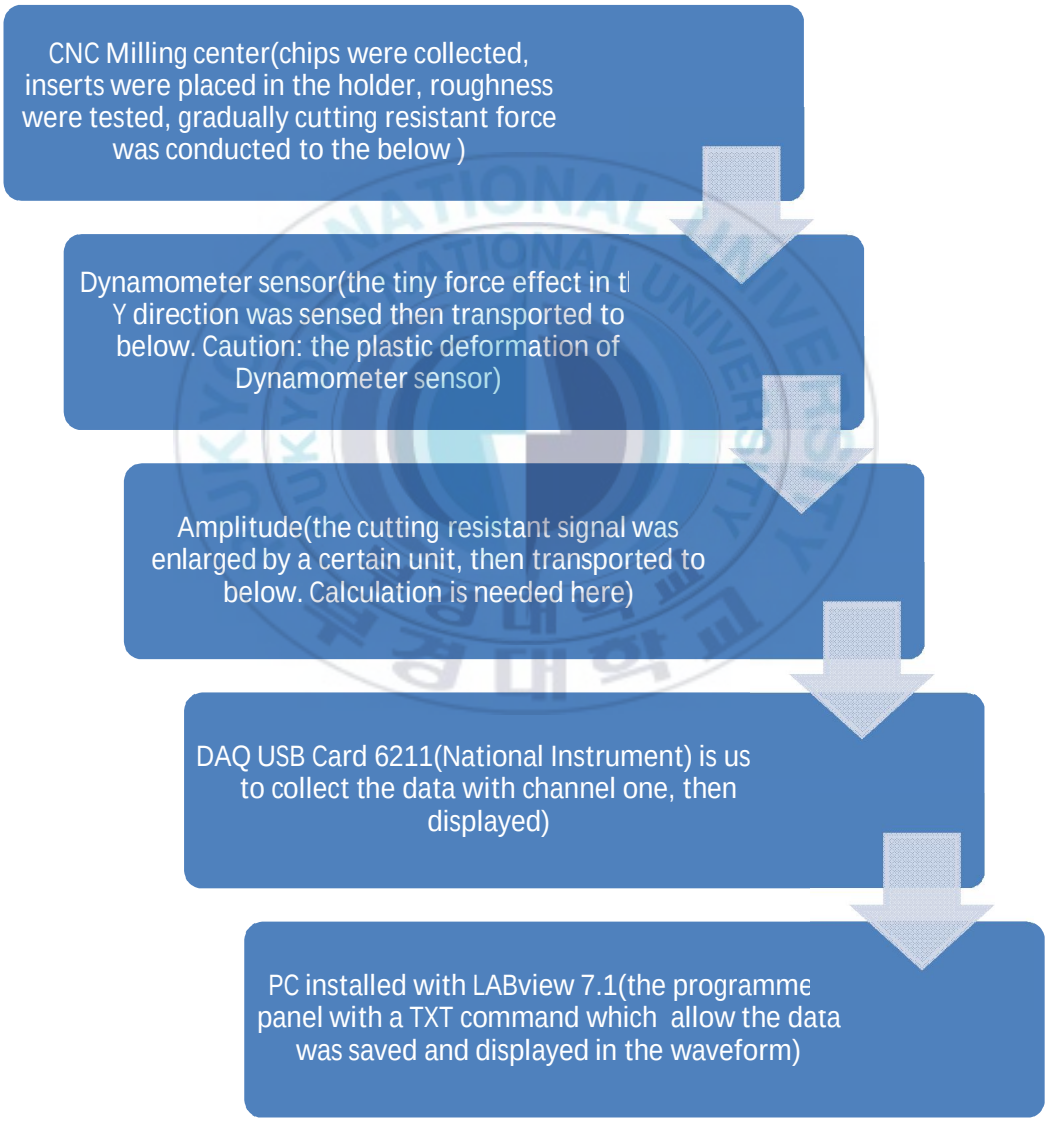

Fig. 12 The main steps of the cutting test

Ⅲ. Result and discussion

1. TiSiCN coating analysis

1.1 Scratch test

In this test, the coated material is placed under a diamond tip which connected with a gradually data-acquisition system, the scratch length and applying load is depend on the coating properties and working condition, the load was gradually increased when the diamond tip attached the coating, the responding of the tip from the surface was reflected to the data-acquisition system, which were recorded along with the load, the friction coefficient was calculated, when the applying load reaches a certain value that the coating cannot withstand, there will be small chips generated from the coating surface, this load value is called low-critical load, with the load increasing, there is significantly scratch observed at the surface and also the signal from the diamond tip show a jump spectrum to a high value, this load is called high-critical load, which means that the coating was completely removed by the diamond tip, the scratch test of three specimens are list below in the Fig. 13~15.

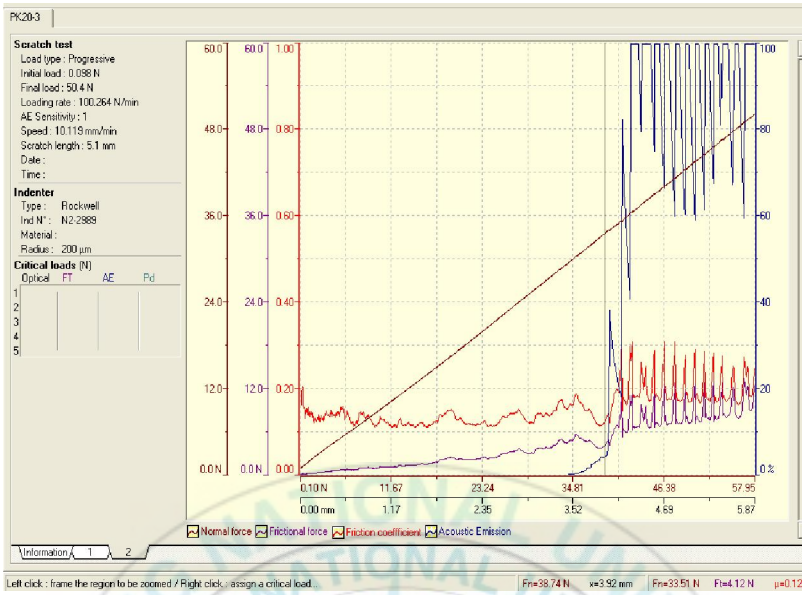

(a) Scratch test result of PK20

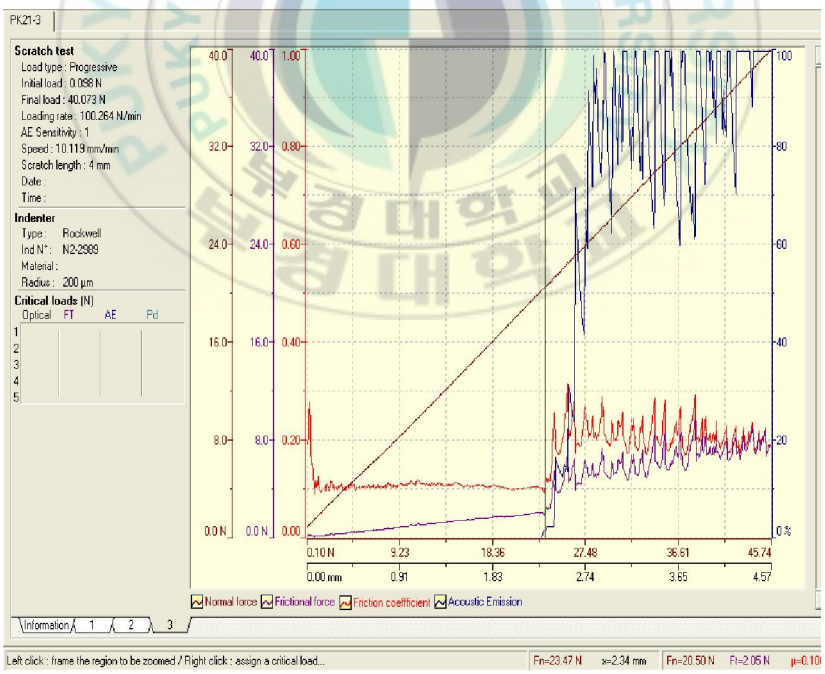

(b) Scratch test result of PK21

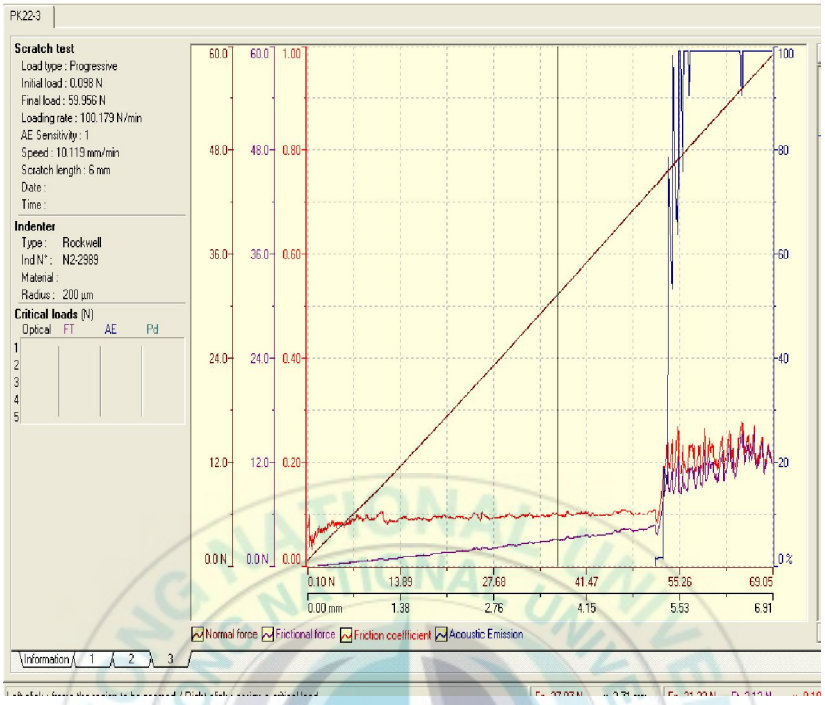

(c) Scratch test result of PK22

Fig. 13 The scratch test of (a)PK20,(b)PK21,(c)PK22

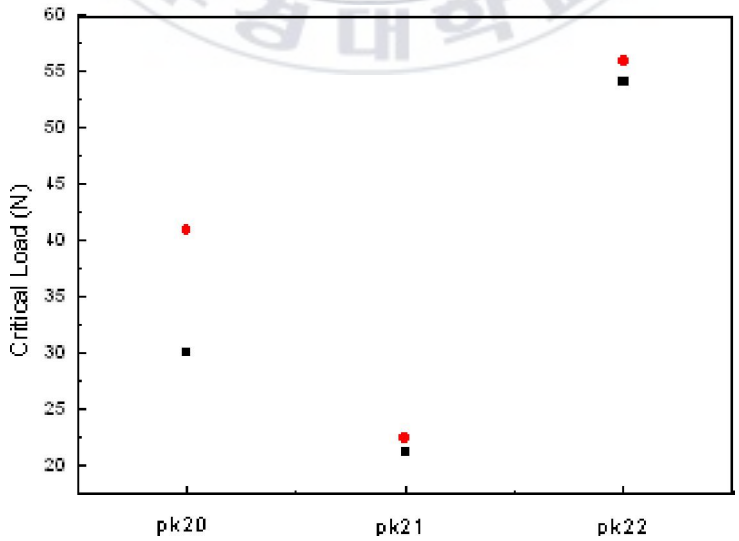

Fig. 14 Low and high critical loads of PK series

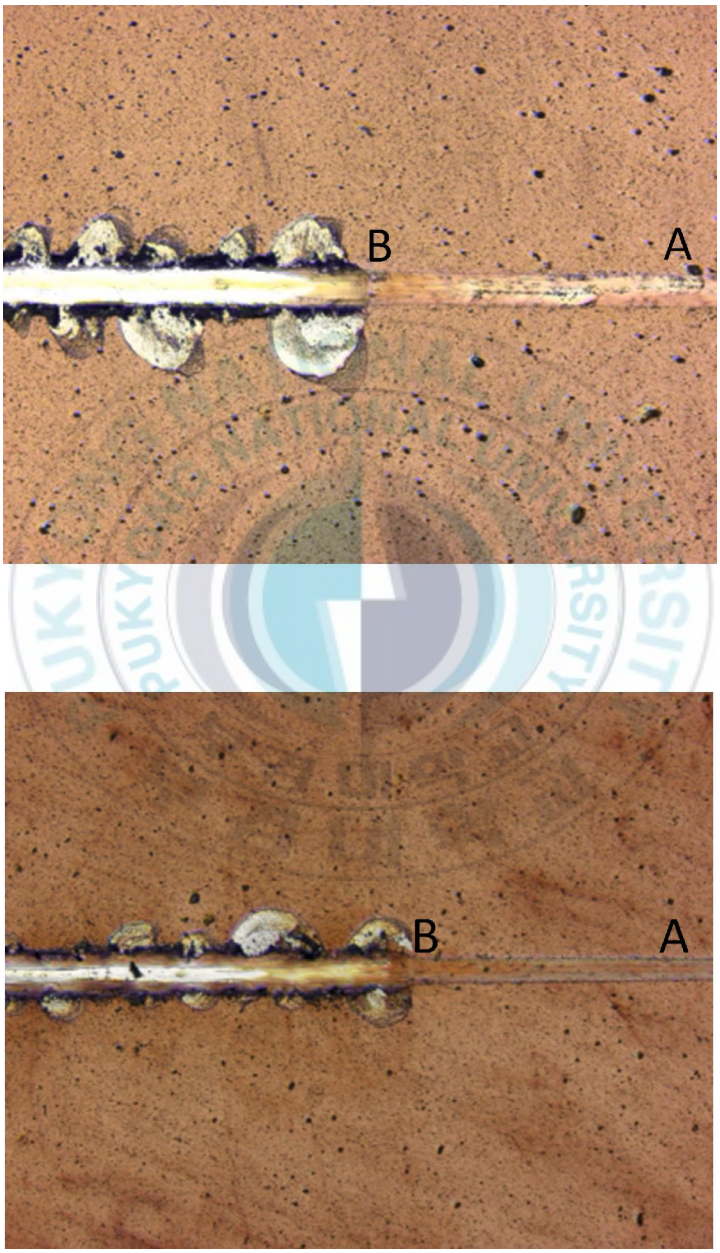

(b) PK21

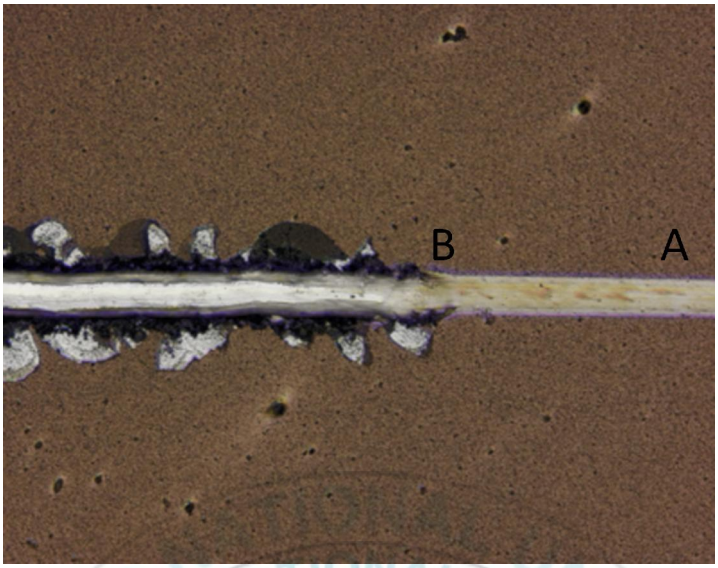

(c) PK22

Fig. 15 Images of scratch failure at the coating surface of PK20, PK21 and PK22 (1.2 mm*1.2 mm)

In this test, the continuously increasing load on the diamond indenter will eventually cause damage to the thin film coating, while the failure limit is reached, a succession of a single shock wave bursts and not a continuous signal spectrum is emitted, by judging the load applied per minute of every 3 tests, we got the average critical load of each test listed as Fig. 14, the scratch images of the three samples were list above in the Fig. 15, in the images, Point A and B are indicating the low critical load and the high critical load where at Point A small chipping occurred and color turned lighter and lighter, at the section of between Point A and Point B, the scratch gradually did damage to the surface where the color turned more lighter which indicated more base material was exposed to outside and lost the protection of coating. At Point B where large delamination occurred and severe coating chipping and totally failure were observed in left-hand side of

Point B. Some tests failed because the final load did not exceed the critical load of the coating. From Fig. 13, clearly, we can see that PK22 shows a highest critical load up to 55 N with a lowest COF around 0.09, and the PK20 shows a relative high COF around 0.14 and a low critical load which indicate a hindering in the dry cutting due to the easily delamination between the coating. It is interesting that the PK21 shows a very low critical load and also low COF at scratch test, as far as we concerned, it is assumed to be accompanied with the deposition parameters which show a high carbon contend in this film, which means TiSiCN coating seems to be more brittle due to the high carbon content, the carbon atoms in the high-carbon contend coating easily diffused to the surface to form as a graphite-like coating to be as a lubricant in the test, however, since the graphite-carbon has a plane atom structure which indicated a very low shear force, it is much more easier to delaminate from the surface at the scratch test, besides a lower cutting force and surface roughness is also expected in the cutting test due to the DLC-like properties [18]. The PK22 show a best performance in the scratch test which is expected to be well-performed in the dry cutting test. In the Fig. 11, we also can see the porosities all over the surface of PK20, PK21 and PK22, it seems that the porosity distribution of PK20 is the highest among three, while PK21 and PK22 are similar looking, directly this high porosity distribution can lead to high surface roughness and bad mechanical properties, such as higher wear and corrosion rate which are not desired in the cutting application.

1.2 AFM test

AFM images usually used to yield the surface characteristics of the film. From the Fig. 16 of the mophology of AFM test, all the PK series TiSiCN coating have finer grain particles, according the image indicating a low surface roughness and low COF we can expect. PK20 grain also seems bigger than the others while PK21 and PK22 grain size is similar.

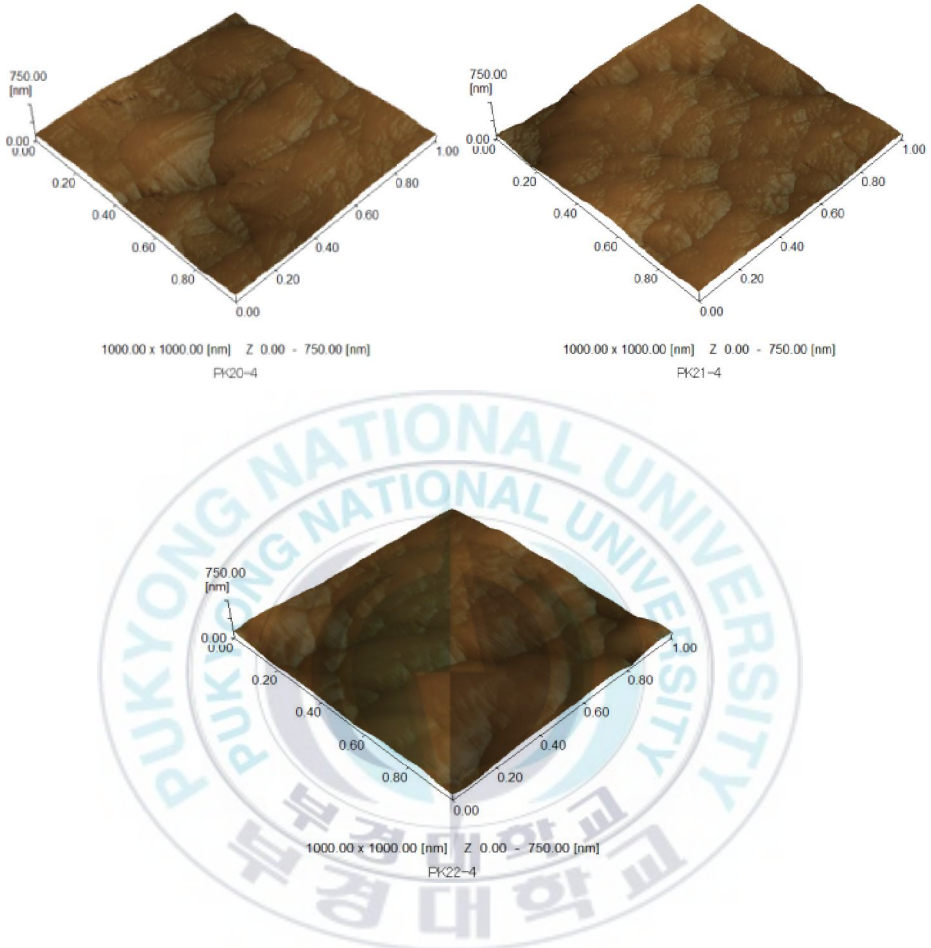

Fig. 16 AFM iamges of PK20, PK21 and PK22 (1um×1um)

In the TiSiCN nanocrystalline structure, the grain size plays a very important part in the mechanical properties associated with carbon contend, as resported the grain size containing 2.1-3.4 at.% Si decreases significantly from 30 to 7 nm, when the carbon concentration increases from 10 to 38.6 at.% [20], ecpecially in this ceramic coating, the size of nanocrystalline is much related to the toughness and ductile properties. Nanocomposite structure with very fine crystalites resulted

in the enhanced of the hardness, grain boundary hardning derived from the increased cohesive energy at interphase boundary along with the percolation phenomenon of amorphous phase is believed to play a role in enhancing the hardness. These size effects are closely related to the increased strain hardening behavior of thin film systems, which is caused by the confinement of dislocation generation and movement within a small volume of grain. Since the model predicts that dislocation densities of thin films increase as the film thickness and grain size decrease, strain hardening due to high dislocation densities can be considered as an important source of thin film strenghening. Yielding strength is maximized with decreasing grain size, ultimately, very small grain sizes make the material brittle. In general, the yield strength of a material is an adequate indicator of the material's mechanical strength. Crack easily propagates along small size grain boundaries or inter-grain leading to low toughness. In grain boundary strengthening the grain boundaries act as pinning points impeding further dislocation propagation. It requires more energy for a dislocation to change directions and move into the adjacent grain, the reasons are:

1. lattice structure of adjacent grains differs in orientation.

2. grain boundary is also much more disordered than inside the grain, which also prevents the dislocations from moving in a continuous slip plane.

1.3 XRD test

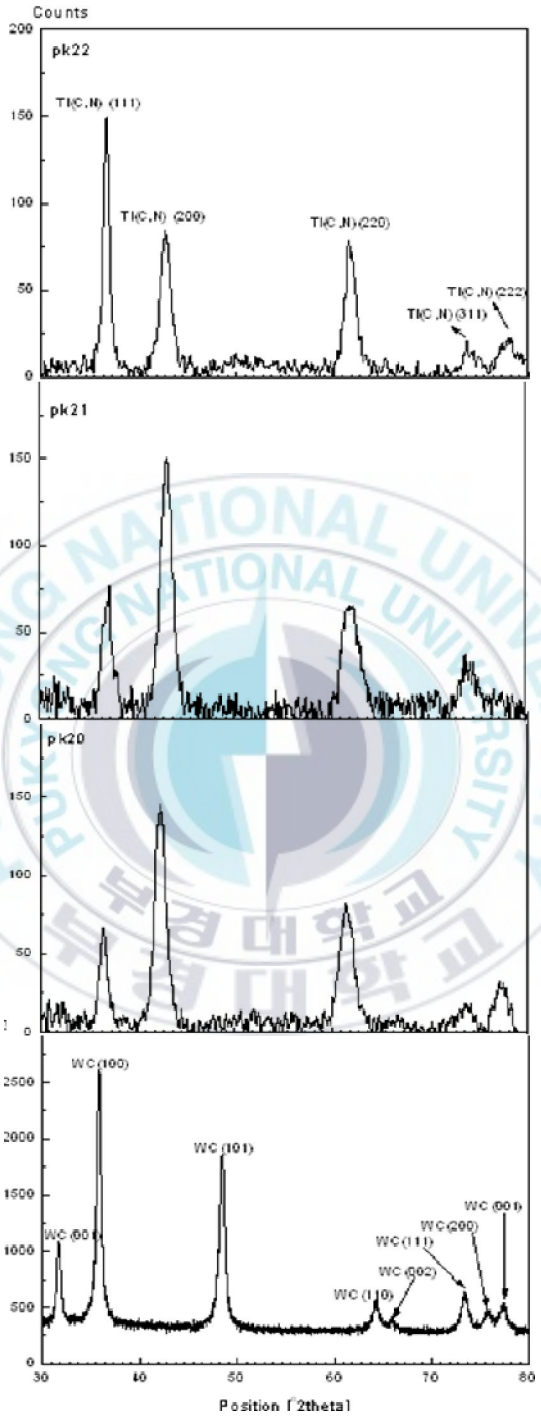

Fig. 17 XRD spectrum of Raw material, PK20,21 and 22

The XRD spectrum listed as Fig. 17 which shows the XRD patterns for the WC-Co and PK20, PK21,PK22 of TiSiCN samples, as we can see from the spectrums, the structure was dominated by f.c.c Ti(C,N) (111), Ti(C,N) (200), Ti(C,N) (220) plane, Ti(C,N) has a same crystalline structure as TiN, but a higher inter-plane D because of the C replacing of N. In the coating, carbon atoms replace nitrogen atoms in TiN crystalline lattice as Ti(C,N) which may increase hardness as a solid solution based on the rule-of-mixtures [23]. PK20,21 have a similar XRD spectrum while the PK22 have a strongly preferred orientation Ti(C,N) (111). All of PK series have a sharp peak indicating fine crystalline structure in the TiSiCN film, however, the broadened diffraction peaks in the XRD pattern may imply that some amorphous structure be incorporated in Ti(C,N) as a solid solution. Although XRD results did not show amorphous Si_3N_4 phase, the possibility that Si_3N_4 could exist in amorphous form was expected [21,24,25], using TEM. The TiSiCN coatings exist as a Ti(C,N) solid solution when the carbon concentration is high (>29.3at.%), and preferred Ti(C,N) (200) crystal orientation appears [26], with a high flow rate of CH_4 and $SiCl_4$, high Si and carbon content, TiSiCN has a mixture orientation [111][220][200] [22], the Si and $TiSi_2$ peaks disappeared when the C contend reaches over 29.3 at.% due to larger number of C replace nitride in the TiN phase, nitrogen exist as an amorphous phase of silicon nitride, more Si was consumed to form Si-N bonding.

According to WEI [27], the nanohardness data of the coating is 42.4 Gpa is much larger than 30 Gpa of TiCN which is deposited under the same PEMS maybe varied with the coating parameter, even though, the super high hardness with a elastic modulus 299.7 Gpa was conducted which indicated a more harder and more tougher coating. Also, the hardness of TiSiCN coatings increases with the increase of C content and achieve the maximum value of about 48 GPa at the content of and 10 at.% Si, and 30 at.% C, the hardness is linearly depending on the Si and C contend, but more closer to the contend of Si [22], the hardness of

TiSiCN decreases when the silicon content exceed 8.9 at.% due to the thickening of the Si_3N_4 phase between crystallites as Si content increased. The maximum hardness and minimum of crystal size achieved at the Si content of 13 at. %, and decreased gradually with the increasing silicon content, due to a diminished nanocrystalline-size hardening affect as larger nanocrystallites emerge [26]. It was found that in the nanocrystalline structured material with a amorphous structure embedded in the matrix, the ceramic coating becomes more ductile and hardly to determine the grain boundary [27]. So, for the nanocrystalline structured thin coating TiSiCN, it needs to be further investigated since:

- The correct assessment of toughness of the thin film required to investigate the system thin film/substrate as one unit because the mechanical properties play a decisive role in the formation of cracks
- The strongest parameter influence the formation of crack is the film structure and its macro stress
- Nanostructured film with X-ray amorphous structure and small compressive macro stress(~0.1 Gpa) are very stable against the cracking even at high value of thin film hardness H_f exceeding 20 Gpa

Since the difference substrate we used, that the nanohardness need to be carried out for the further study in the macro-indentation, the crack and precise value should be conducted later.

2. CNC face milling

2.1 Cutting resistance force and roughness

The following Fig. 18 shows the cutting resistant force. The feed direction is the same as the rotation direction to get high impact load during cutting since every circle of rotation of the teeth which is a very severe cutting condition.

The holder d=50mm, Type: TaeguTec HP90T 50R-22 15450,

Feed speed: 150 mm/min, RPM: 3000, we placed only one insert in the Four-Tips holder, so the feed for every teeth: 0.05mm/rev

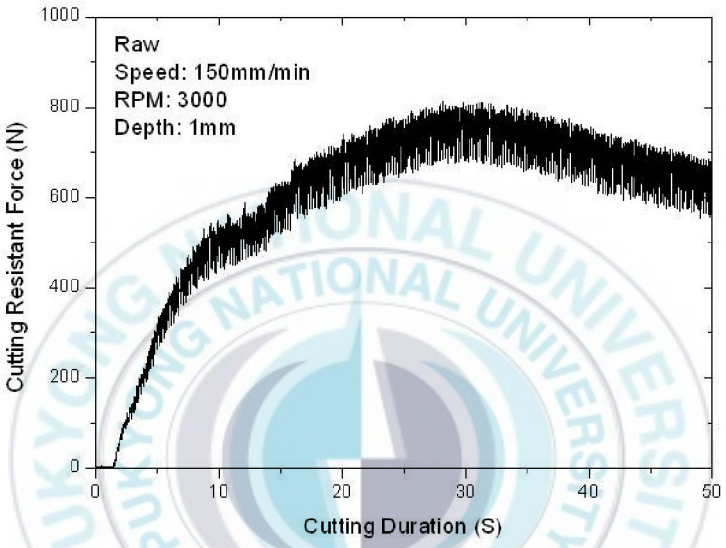

(a)Uncoated

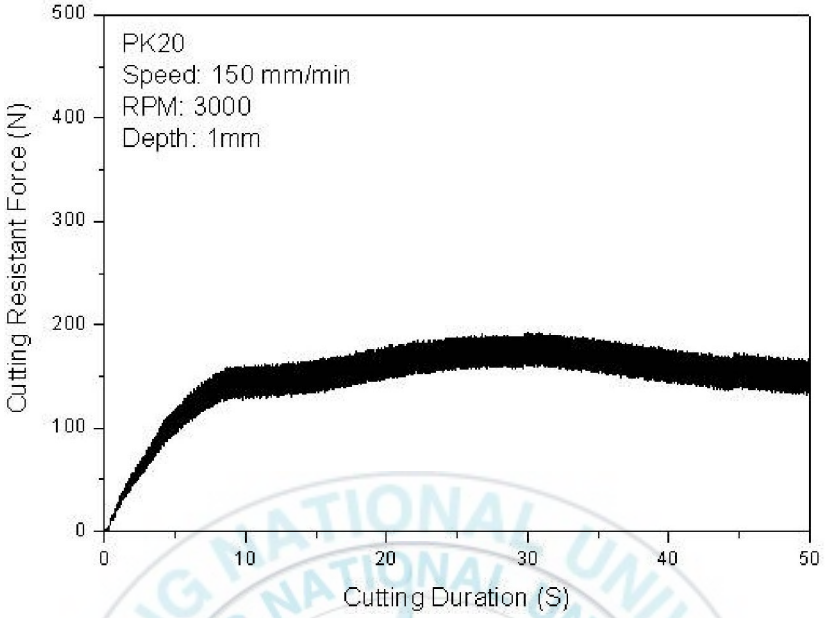
PK20
Speed: 150 mm/min
RPM: 3000
Depth: 1mm
Cutting Resistant Force (N)
Cutting Duration (S)
0
100
200
300
400
500
0
10
20
30
40
50

(b)PK20

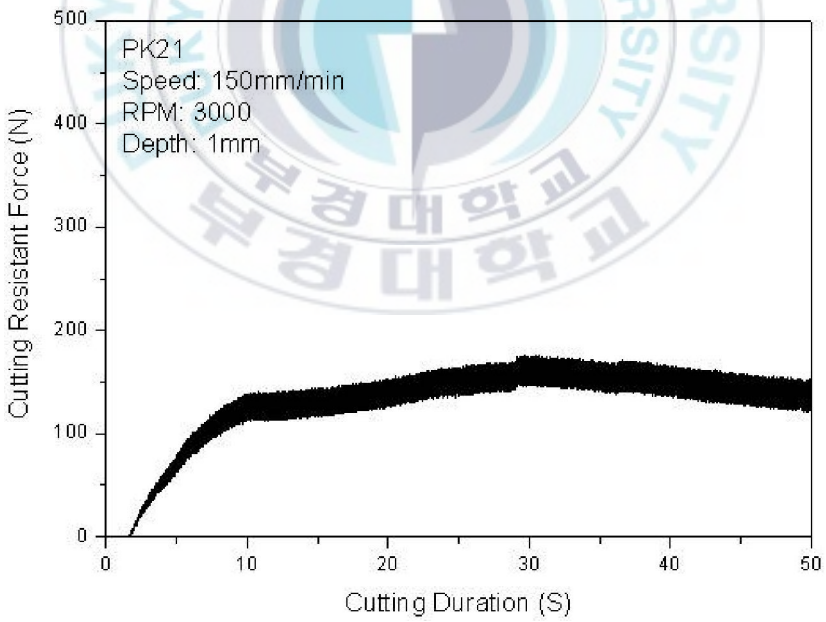
PK21
Speed: 150mm/min
RPM: 3000
Depth: 1mm
Cutting Resistant Force (N)
Cutting Duration (S)
0
100
200
300
400
500
0
10
20
30
40
50

(c)PK21

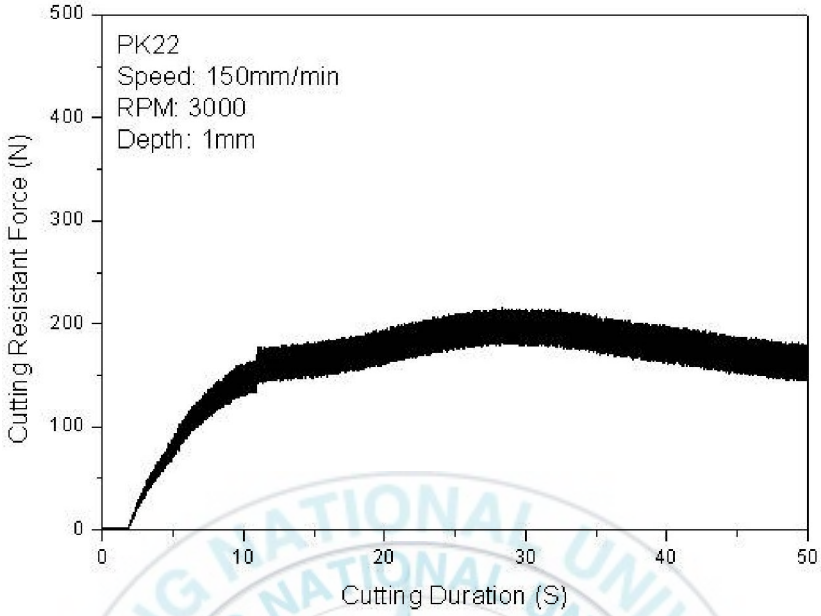

(d)PK22

Fig. 18 Cutting resistant force of (a)Uncoated, (b)PK20, (c)PK21, and (d)PK22

During the cutting test, the real temperature is very difficult to be assessed, this is the reason why a lot of research groups employ FEM and similar methods to give indication of the values [28~31], however, in the section of chip formation, the temperature at the cutting zone will be assumed according to the color of the chips since at the dry machining, more than 80% of generated heat is carried out by the chips.

As can be seen in the Fig. 18, the cutting graph shows a similar trend that at the beginning of the cutting, the cutting force largely increased with time, and then gradually increased with time maybe because the surface contamination served here to increase the friction, and as the contamination was removed out, the cutting force was decreased gradually. Test time was short and we collected the

data of the beginning period, since one insert was placed in the holder, high impact load and high contact pressure was conducted at the cutting zone, so, all the PK series show a relatively tip breaking process corresponding to the little jumping of the cutting force, even so, the cutting force was detected at the raw material is over 1000N and it kept rising continuously along with time, while the PK series show a relatively low cutting force and a low magnitude of vibration compared with the raw material, PK20,22 show little higher cutting resistant force than PK21 mainly due to the lower surface roughness and carbon contend while in the cutting zone under low temperature, transferred graphite-like carbon is the main lubricant in the contact surface, as seen from the critical load discussed before, the PK21 shows a very low critical load which indicates a very low tool life in this severe cutting condition, it is not observed that PK 21 is completely failed since the data was collected at the very beginning at the cutting test. Among the PK series, the PK22 shows a lower cutting force and lower magnitude of vibration indicating a outperforming properties in the dry cutting of median carbon steel without a lubricant, it should be serious noted the work from Shiya Imanura [32], deposited by cathodic-arc ion plating, he and his coworkers did cutting test with the same workpiece as in this thesis, obviously, he chose the multilayer(TiAlCrN/TiSiCN) rather than single layer(TiAlN) since he found that the compressive residual stress is significantly high up to 5.3 Gpa even measured thickness is around 5nm(the thickness of the TiAlCrN is less than 50nm), the multilayer can reduce the stress and also increase the hardness around 40~50Gpa while a single TiAlN's nanohardness is below 40Gpa, as one research work which is the only one related to the dry machining on the carbon steel, the column structure of base material TiAlCrN is considerably degrade the mechanical properties while as bonding layer mainly due to the deposition process, while if apply heavy ion bombardment in this work, column structures are eliminated , up coating hardness is much high while this is interesting that in conversional multilayered coating, the coating consisted as hard coating below a lubricant coating, here, the researcher put the TiSiCN coating as a hard and also a lubricant

coating while the other layer only served as a bonding layer. Besides, the drilling is applied while as described before, dry drilling is the most severe test of coating under dry condition since chips which are expected to carry away most of the generated heat are hard to remove out.

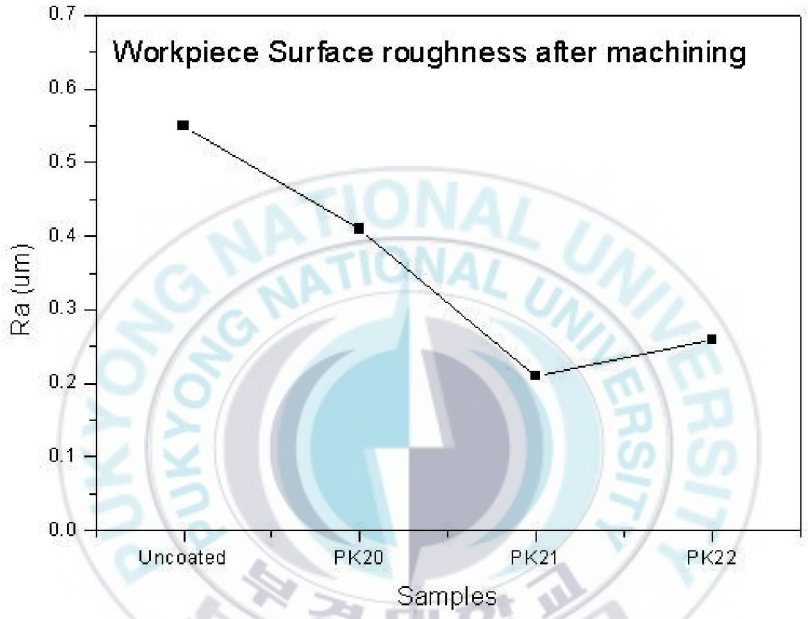

Fig. 19. Surface roughness of PK series and Uncoated cutting inserts

After cutting test, the workpiece was test using Surface Roughness tester, the result was list above as Fig. 19, it can be found some evidence for the properties of PK series, according to the result list above, the raw material shows a highest surface roughness which may be caused by serious oxidation degradation of WC-Co, and up to 0.65 of Ra was observed, PK20 and showed a relative high surface roughness while PK21 shows a lowest surface roughness corresponding to the cutting force, maybe PK21 has the most highest carbon contend that in the cutting test, the carbon diffused to the surface as a transfer layer to reduce the

friction, surface roughness of PK22 is just a little higher than the surface roughness of PK21. Actually, the result is relative high considering the precision machining, the reasons may be the one insert was placed in the holder which caused the high cutting length per revolution, in the surface of workpiece, cutting tracks were clearly observed while at the high feed, the cutting tips can't cut closely, this led to surface asperities and high surface roughness, the result should be better by applying 4 inserts or lower cutting feed. The following SEM on the edge will show more detail information of the adhesion and element transformation.

2.2 Wear Analysis

Tool wear plays the most important role in the tool life, there are various of tool wears such as: adhesion: High pressure/temperature cause adhesion of asperities between the tool and the chip. Abrasion: Hard particles in the workpiece cause abrasion of the tool-- Dominant mechanism for flank wear. Here, in this study, the adhesion wear was studied, after dry cutting, the tips are sent to be examined under SEM, the Fig. 20 shows images of the raw material.

The first group shows images of uncoated tip after dry cutting median carbon steel, as we can see from the first image, the tip is extremely serious damaged, and large part of the cutting edge is lost due to the adhesion contaminations and the high impact load, from the element analysis, we can see that Fe has a severe adhesion to the WC-Co tip, and covers the cutting edge, WC-Co was expected to be serious degraded by oxidation and maybe few ferrous oxidation is also observed at the cutting zone.

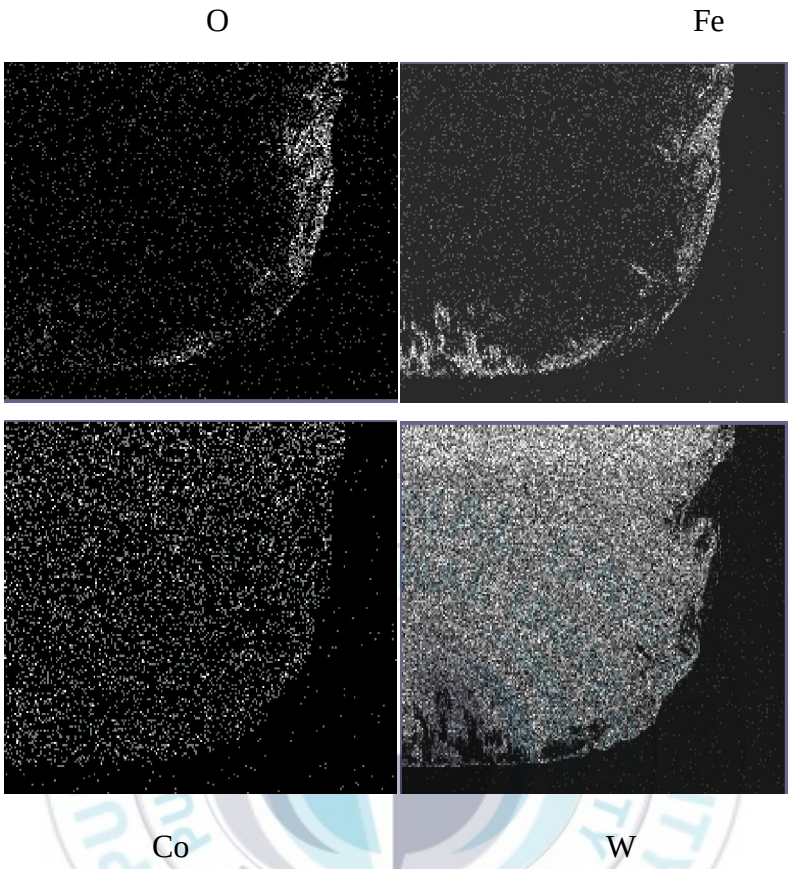

Fig. 20 Rake face elemental mapping of WC-Co

In the WC-Co, the main wear mechanism is abrasion and adhesion wear, while the abrasion wear is due to the hardening of material during cutting, with the temperature higher, the ships erode the rake face to form crater wear which cause more severe wear rate.

As reported by A.Devillez [33], Al_2O_3 was detected while applied TiAlN, served as thermal protection layer, Al_2O_3 is a conventional CVD coating which has a outstanding wear resistance and superior thermodynamic stability, the Al_2O_3 resisted the chemical dissociation and dissolution reactions that dominated the metalcutting wear process at a high cutting speed, however due to the brittleness of the Al_2O_3, it mainly is used to light duty, low stress cutting operation [34]. The

oxidation material was expected to form during cutting in TiSiCN is silicon oxide, according to the elemental mapping, the silicon diffused from the coating at around 250°C [22,25,26], to form SiO_2 which will enhance the thermal conductivity, the cutting temperature in the dry cutting was hard to investigated but assumed to below 600°C, while as everyone knows beyond the 600°C, the Ti will diffused to the surface the form the $Ti0_2$, which is n-type semiconductor with oxy vacancies and the Ti interstitial as the pre-dominate defects, it is porous and non-lubricous rutile-type coating, working function studies indicate that the defect structure within the boundary layer of TiO_2 consists of a variety of complexes and clusters. It is has been shown that Fe segregates to the surface of $Ti0_2$, it has been suggested that the electrostatic predominates in Fe segregation since the ionic of Ti(4+), and Fe(3+) ions are comparable(68,64 pm, respectively) [35].

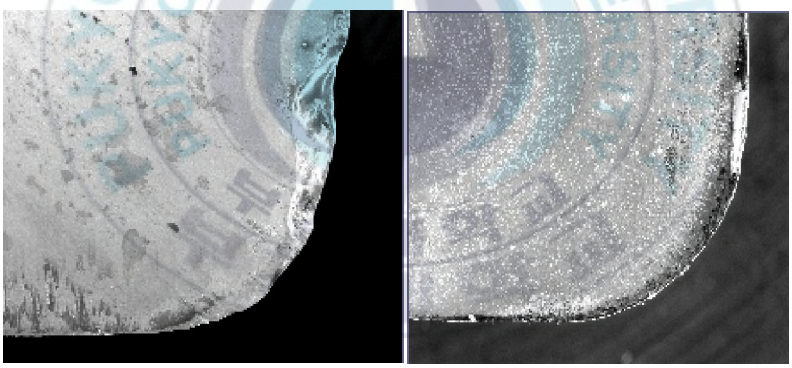

(a) Uncoated (b)PK20

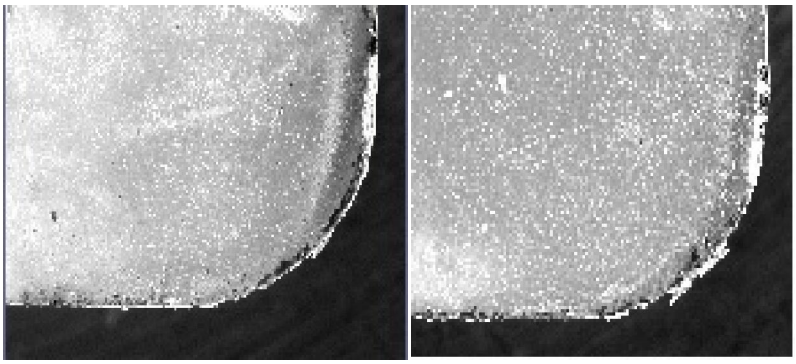

(c)PK21 (d)PK22

Fig. 21 The length of missed part in PK series.

In the Fig. 21 shown above, even some cutting tips were missed during the cutting, the cutting force and surface roughness shown before indicates little effect to the cutting performance, while PK 22 has a shortest length about 50um shown in the Fig. 21(d), the tip-breaking process is really a problem since only one insert tip in the four-inserts-tip holder, due to the high impact load and much more severe cutting condition compared with the real industry cutting conditions, the high impact load and cutting feed is 4 times than the real industry application, even though, it is a problem that kind of material missing in machining, as we expected the TiSiCN has a rather high hardness and also amorphous structure was embedded in the nanocrystalline structure which indicate a more ductile ceramic than other conventional ceramic coating, it seems that it is still a main work that we need to improve the toughness or the fracture toughness need to be evaluated, the black one along the cutting edge is not oxidation but the effect of the background color.

From the image of PK series shown in the Fig. 22~24, similar elemental mapping characteristic was observed, highly distributed Si was observed at the cutting edge, indicating the Si diffusion to the surface forming as a oxides which

served as a lubricant, a little Fe adhesion was observed and Ti disappeared at the cutting edge but W was appeared indicating the coating maybe delaminated from the surface.

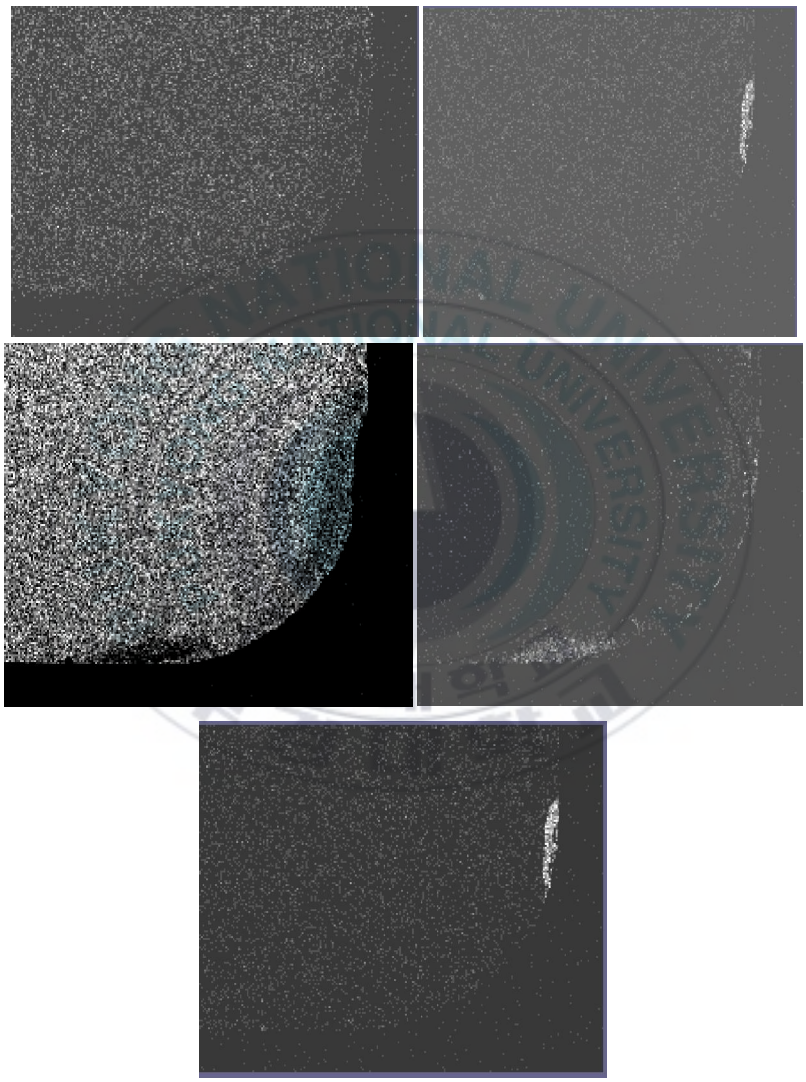

Fig. 22 PK20 elemental mappings of N, Si, Ti, Fe and W in turns

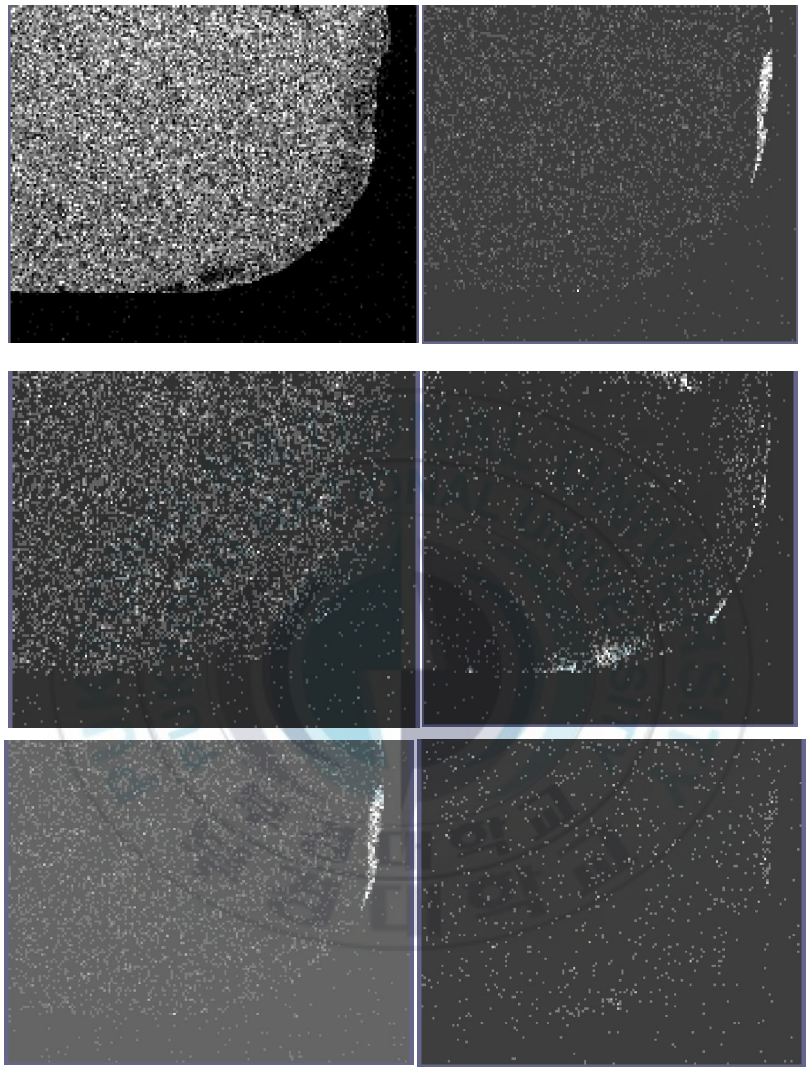

Fig. 23 PK21 element mapping of N, Si, Ti, Fe, Co and W in turns

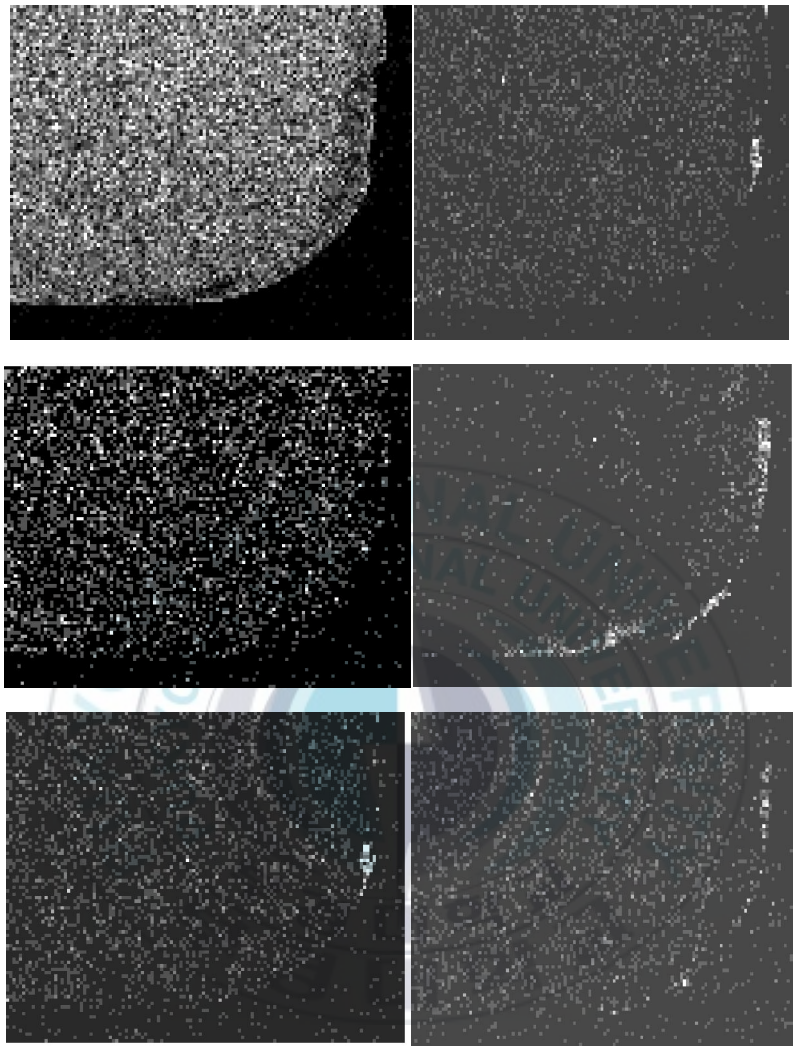

Fig. 24 PK22 element mapping of N, Si, Ti, Fe, Co and W in turns

All of the PK series show a very good anti-adhesion properties to steel in cutting median carbon steel, as discussed before, Built-up-edge (BUE) forms is prevented between workpiece and the tool since it becomes unstable due to the very well anti-adhesion properties by applying Ti in the coating [36], little adhesion of Fe was observed in the PK series indicating very good anti-adhesion

properties, while the cutting performance is revealed in the work of Shiya Imamura [32], even under dry drilling, TiSiCN coating can significantly prevent from oxidation wear so that the cutting edge temperature will not increase, it performed excellent tribology properties since the coating contains carbon. Providing a lubricated layer TiSiCN film on the surface will significantly increase adhesion resistance. While in this work, PK22 show a outstanding cutting performance with a very well anti-adhesion properties and also shortest missing part of the cutting tip. In the machining, the humidity is also a important factor according the work of H. Xu [37], under the same deposition technique PEMS, the coolant could prevent the adhesive wear which dominate the wear behavior of coatings against soft aluminium pins in air. While in the coolant, TiSiCN coating is found to be higher COF than TiN coating whether against alumina or aluminium, that means the TiSiCN are suitable and only suitable in the dry machining while TiN coating can perform better in the coolant.

2.3 Chip formation

Chip formation affects the surface finish, cutting force, temperature, tool life and dimensional tolerance. A chip consists of shiny side (flat, uniform) and the other side is the free workpiece surface that has a jagged appearance due to shear. Tresca [38] published a visio-plasticity picture of a metal cutting process. He gave an opinion that for the construction of the best form of tools and for determining the most suitable depth of cut, the minute examination of the cuttings is of the greatest importance. He was aware that fine cuts caused more plastic deformation than heavier cuts and said this was a driving force for the development of more powerful, stiffer machine tools, able to make heavier cuts. At the same meeting, it was recorded that there now appeared to be a mechanical analysis that might soon be used – like chemical analysis – systematically to assess the quality of formed metals.

(a)Uncoated

(b)PK20

(c)PK21

(d)PK22

Fig. 25 Cutting chips of (a)raw material, (b)PK20, (c)PK21, and (d)PK22 in turns

Fig. 25 shows the chips of raw material with the PK series. This type of discontinuous chip is usually formed when cutting hard or brittle materials, partly because these median carbon steel can't withstand high shear force and therefore the chips formed shear cleanly away. However, the chips formed may be firmly or loosely attached to each other or may leave the cutting area in a fine shower – as often encountered when cutting hard Brass. For the chip formation process, there are two theories which are crack theory and adiabatic theory, first one initiated form a crack which is propagated by high shear stress, the other is a thermal plastic instability occurs within the primary shear zone and the mechanism of deformation is the one in which the rate of thermal softening exceed the rate of strain hardening [39].

The minimized formation of built-up edge on the PK series tool surface led to the cutting edge sharp. As a result, the improvement in machinability and the machined surface of the work materials are in high quality. These properties are also observed from the chip formations where we can understand that chips were removed favorably. The removed chip shape prevents the work material from being scratched by chips, and the machined surface caused by re-adhesion to the work material. Consequently, the cutting life of the tool had been successfully lengthened. Even in dry machining, coated tools had excellent advantage over uncoated tools for median carbon steel cutting. It is clearly can be seen that for the chips from the uncoated raw material were dull and irregular surface in appearance, and had a large curl diameter, they chips seems dark and gray which indicated oxidation at the cutting zone where large heat generated. While for the TiSiCN series which assumed to have low friction coefficient had a metallic shine and smooth surface, and were small and curled into a spiral, in contrast, the chips

from PK21 is relatively different from others, small part of the chips are large curl in diameter, and some gray color was observed at some chips which indicated that corresponding to the low critical load of PK21, the coating was partly delaminated and high local temperature was generated at the cutting zone which led to a oxidation of chips. The temperature was not measured but assumed less than 700°C at which Ti will defuse to the surface and for TiO_2 none-lubricant layer, at this high temperature up to 850°C, Yan Guo, et al [40] did research on the oxidation resistant of TiSiCN deposited by Plasma-enhanced chemical vapour deposition, he found that the coating hardness, surface roughness, chemical composition and surface morphology are strictly relative to the Si content, with the increase in the Si content from 4.3 at.%, 7.4 at.%, to 11.6 at.%, the hardness is increasing from 43Gpa, 49Gpa, 52Gpa, while the hardness and surface roughness were slowly decreased while under the temperature of 750°C, 800°C, 850°C by formation of Ti oxide and SiO_2 along their grain boundaries, by increasing the silicon content, the formation of $TiSi_2$ can significantly retard inward diffusion of oxygen because of the consumption of the oxygen, higher silicon content can lead to high volume of SiO_2 higher, which served as a oxygen diffusion barrier.

2.4 Vickers Indentation Test

Considering the data list above, the result of cutting force is relatively high(around 200N) maybe due to several reasons such as low adhesion strength or high impact load which caused the delamination of coating and the cutting process is carried on with unprotected tools or partial-missed tools. The high impact induced crack propagation may lead to part fracture of coating. In order to examine the resistant of plastic deformation and the crack propagation resistant in the surface of the coating, the micro-hardness and indentation-induced fracture method are applied. Even the hardness and fracture toughness properties was

evaluated in the paper of WEI [27], due to the difference of the substrate, thickness of the coating and the deposition condition, the result may vary a lot. In this test , the main goal is to analyze the Vickers Indentation hardness and the indentation-induced fracture by different calculation methods invented by various researchers, substrate effect, and crack formation process will be studied. This test was carried on in the Micro-Hardness Tester(Mitutoyo Corpoartion, HM 123) machine, eight specimens was used including the WC-Co based PK20,21,22, raw material, and Stainless steel based PKSS20,21,22, raw material(under the same deposition condition with PK20,21 and 22 in turns).

For this ceramic brittle material coating which ranged several micrometers, there has been increasing interest in the application of indentation fracture mechanics as a simple technique for evaluating various mechanical properties [41,42]. First, in order the reduce the specimen effect in the test such as stress concentration rate and indentation depth effect, the coating thickness and surface roughness are measured using SEM Cross-Section method and Surface Roughness Tester, the results are listed below in the Fig. 26 and Fig. 27.

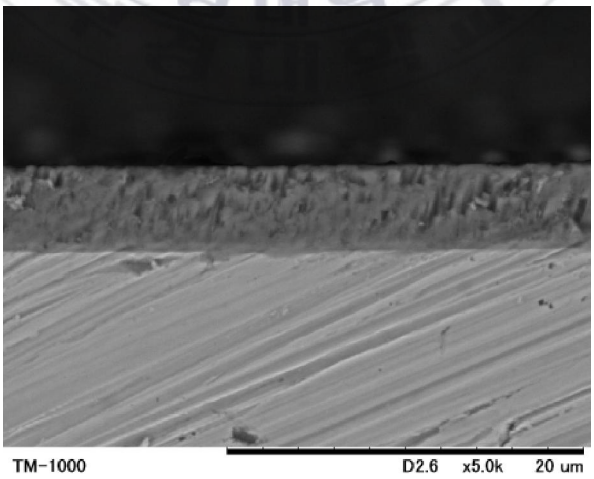

(a)PK20

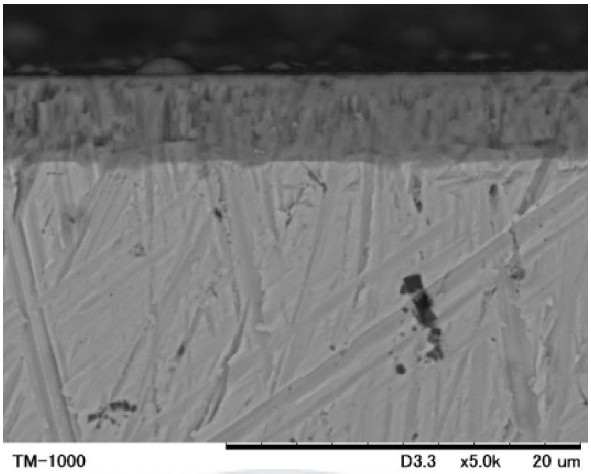

(b)PK21

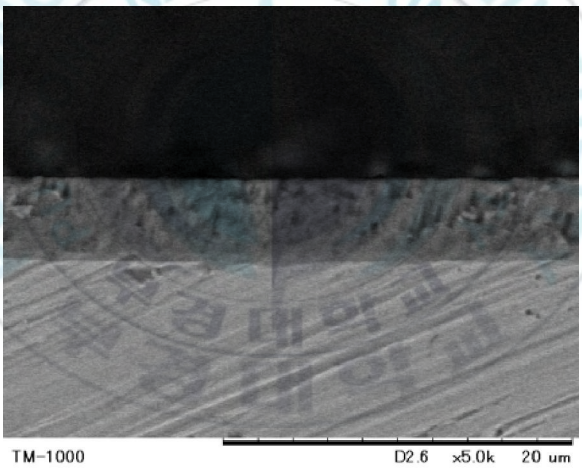

(c)PK22

Fig. 26 Cross-section Images of PK series

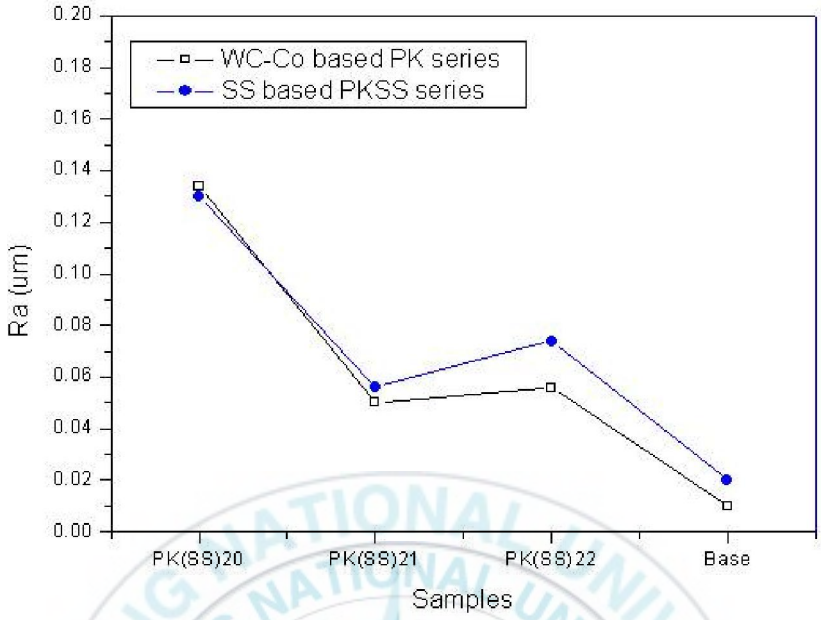

Fig. 27 Surface Roughness of PK and PKSS series

From the images caught by SEM Cross-Section method, the coating thickness is measured around 5 um which is a thicker one compared with typical thin film ranged less than several nanometers, we controlled the indentation depth less than 10 percent of the coating thickness in order to reduce the effect of the base material. Here, by calculating the D1,D2 with the angle 136 degree of the indenter and conditions that the Vickers Hardness Tester used, we applied 50g to examine the Vickers hardness and 500g to examine the fracture toughness. Besides, the surface roughness of PK and PKSS series revealed that the TiSiCN coating inhered part of the mimic properties to the substrate as introduced amorphous structures in the coating, with lower surface roughness substrate compared the Stainless steel in the substrate, the surface roughness of TiSiCN coatings showed also lower surface roughness. Among the TiSiCN coatings, the trend is the same, PK(SS)21 coatings show the lowest surface roughness while PK(SS)22 show higher and PK(SS)20 show the highest surface roughness which means PK(SS)21

showed less surface stress effect. When making indentation on the surface, the high probability of big asperities in the PK(SS)20 leads to much more asymmetric plastic deformation, along with the remove of indentation load, the elastic recovery is also asymmetric which led to less accuracy to analyze the fracture and hardness value.

The Vickers Hardness was obtained under the condition of 50g load, 30s loading and five times for each specimens, calculated the mean value of hardness, and list the result below in the Fig. 28.

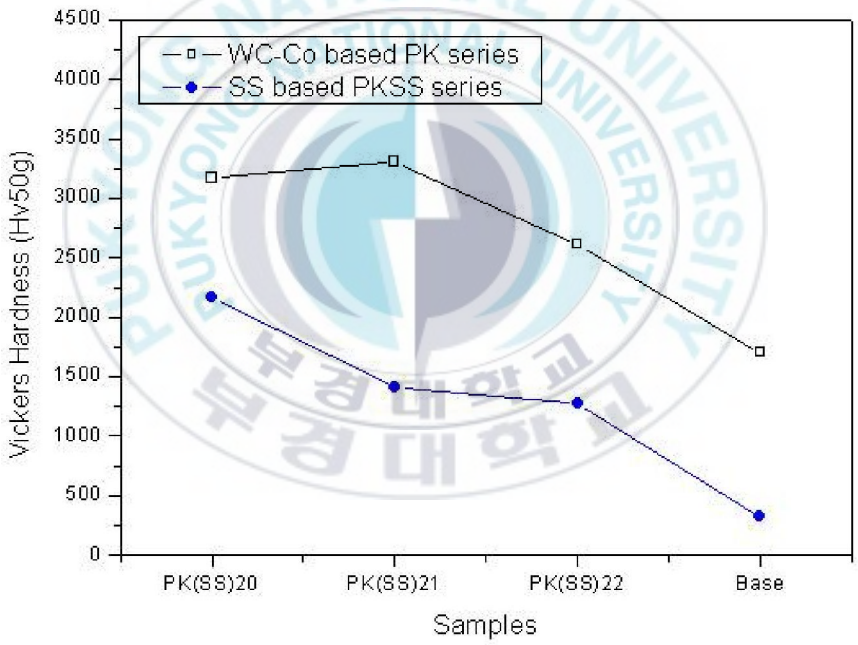

Fig. 28 Vickers Indentation hardness of PK and PKSS series under 50g

Here, from the Fig. 28, the substrate effect is so large that the Vickers hardness value can vary much, according to the result list above, the trend of TiSiCN is almost the same except 21 series(PK21, PKSS21) and with the same base material,

the WC-Co based PK21 ranged first around 3500Hv while stainless steel based PKSS21 ranged second around 1500Hv, stainless steel can largely decrease the hardness of carbon-rich TiSiCN need to be investigated, the reason maybe the relative high indenter load applied on the surface of PKSS coating, while there is big difference in hardness between coating and stainless steel, there is much more likely to cause crack even under low applied load, even we can't see the crack under the optical microscopy under 1000 magnification, there assumed to be cracks along with the indentation, so, that is also a reason why the hardness decreased a lot while coated on the SS.

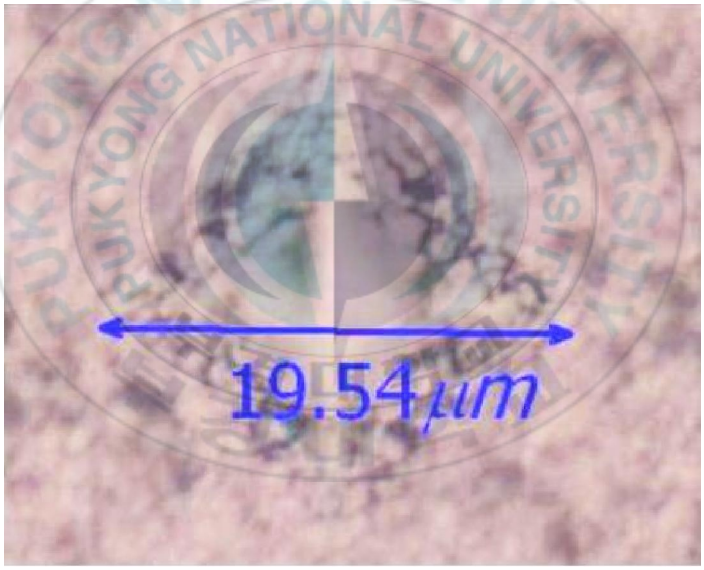

Fig. 29 Vickers indentation result of PK20

The Vickers indentation test results of six specimens were list below as Fig. 29, 30 and 31 using the load of 500g. In Fig. 29 which shows the indentation mark of PK20, it is failed to see any corner crack maybe due to the high surface roughness which cause serious stress concentration, the cracks are likely to propagate within

the indentation along with the grain boundaries and we also can see that even under such high indentation stress caused by diamond indenter, the TiSiCN grain seems not fragile but sink to cause plastic deformation of base material, the likely column structures may assume to be proved here.

The Vickers Indentation results of PKSS series were listed as Fig. 30 below, in these three specimens, the indentations seem similar with a common characteristic of corrugation and edge crack, also no corner cracks were observed in these indentations, this may caused by the high difference of hardness between coating and base material, the indentation energy caused by diamond indenter is much more easier to cause plastic deformation of base material than cracked in the surface, it is assumed that decline crack propagated in the interface between the coating and the base material. When we focused the inside of the indentation, the edge crack and column-structured sinking is also observed here, due to the very low hardness of stainless steel, the soft base material absorbs major of the indentation energy to cause shearing and plastic deformation.

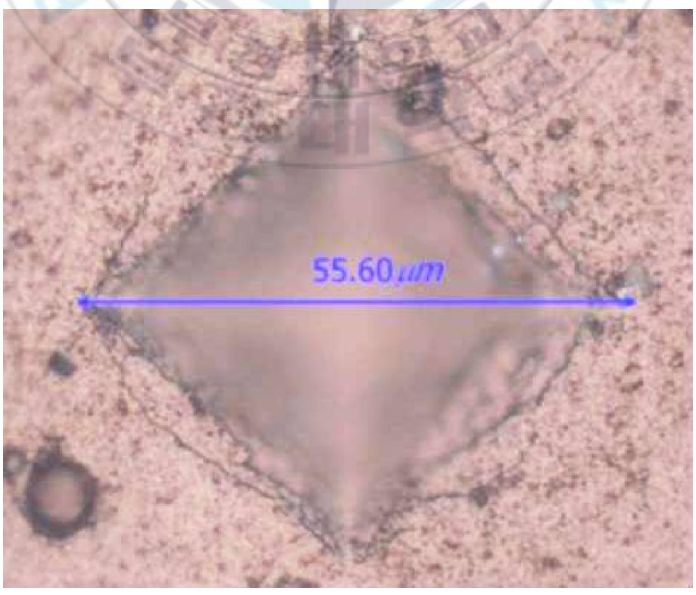

(a)Indentation of PKSS20

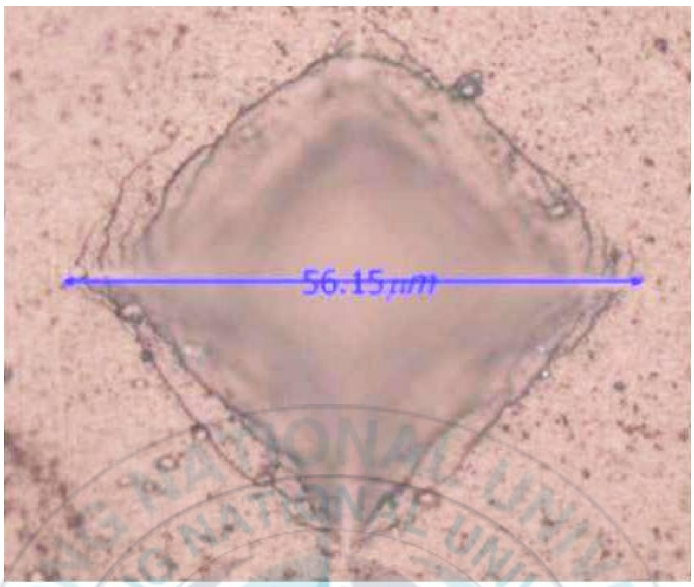

(b) Indentation of PKSS21

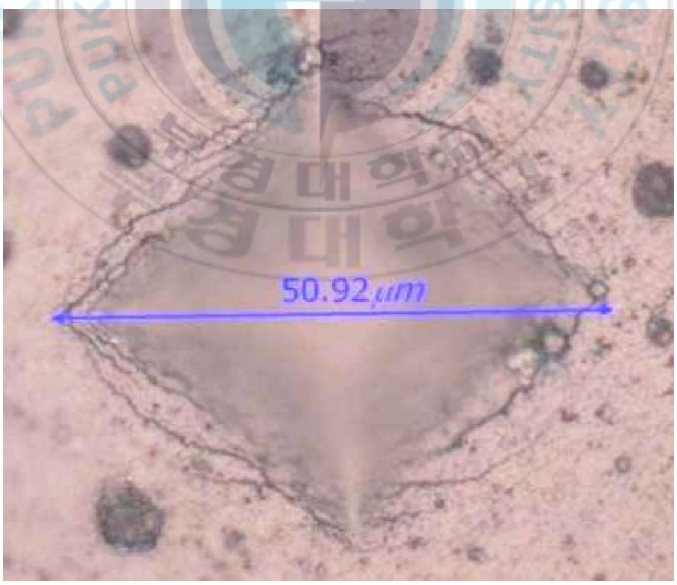

(b) Indentation of PKSS22

Fig. 30 Vickers Indentation results of PKSS20,PKSS21 and PKSS22

In the Fig. 31, the PK21, PK22 both showed a fine corner crack at the indentation corner which give a chance to apply the indentation-induced fracture method, the D1 was measured and Palmqvist crack length C was measured, too. The elastic modulus is not measured by assumed around 300 Gpa [27], the Vickers hardness as measured is 3308.8 Hv(50g), 2608.6 Hv(50g) respectively for PK21 and PK22.

So, for this ceramic thick coating which performs brittle manner, it is suitable to apply Linear-Elastic Fracture Mechanics(LEFM), there are numerous works studied on this subject which supplied many methods that we can apply. Evan and Charles uniquely characterized the surface radial cracks in brittle materials generated by Vickers Indentation, their analysis successfully spanned a large range of fracture toughness K_{1c}, the modification of the Evans-Charles analysis was made by Lawn et al on the basis of a more fundamental approach for median/radial cracks [43].

$$(K_{1c} / Ha^{1/2})(H / E)^{1/2} = 0.028(c / a)^{-3/2} \quad \cdots\cdots\cdots\cdots\cdots\cdots\cdots\cdots\cdots\cdots \text{(Eq. 2.4.1)}$$

Where H is hardness, a is indent half-diagonal, E is elastic modulus, and c is the radial crack size. Niihara modified the analysis of Evans and Charles and Lawns by incorporation Palmqvist cracks, rather than median cracks, at a low crack-to-indent ratio size.

$$(K_{1c}\phi / Ha^{1/2})(H / E\phi)^{2/5} = 0.035(l / a)^{-1/2} \quad \cdots\cdots\cdots\cdots\cdots\cdots\cdots\cdots\cdots\cdots \text{(Eq. 2.4.2)}$$

Where ϕ is constrain factor ($= H / \sigma_y \approx 3$), l is the Palmqvist crack. By applying this mode, the K_{1c} of PK21, PK22 are $3.37\ Mpa\sqrt{m}$ and $3.25\ Mpa\sqrt{m}$ respectively.

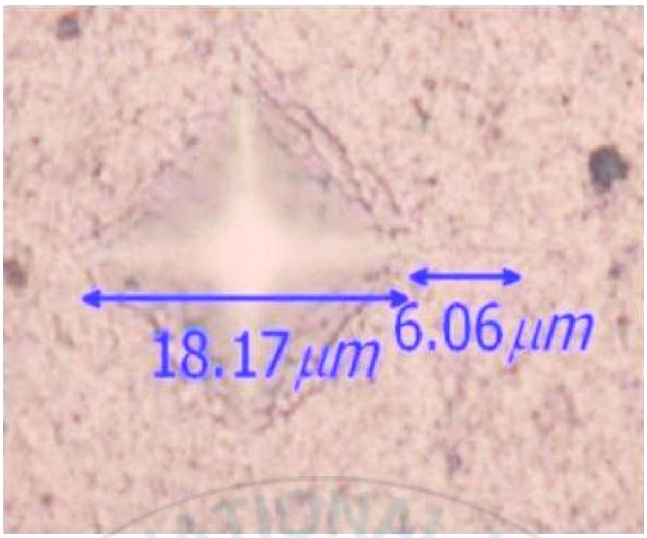

(a) PK21

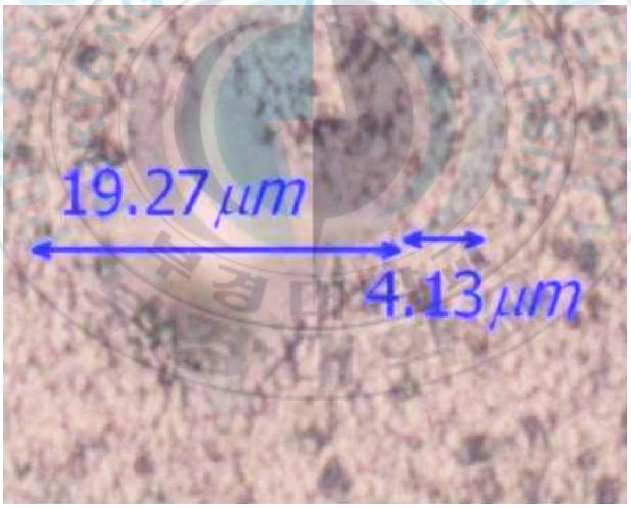

(b) PK22

Fig. 31 Vickers Indentation results of PK21 and PK22

Anatis et al [44] examined various glasses(glass-ceramic, soda-lime, lead alkali), polycrystalline Al_2O_3 and sapphire, Si_3N_4, SiC, Ca-PSZ ZrO_2, Si, and SiC/Co and concluded that:

$$K_{1c} = (0.016 \pm 0.002)(E/H)^{1/2}\frac{P}{c^{3/2}} \cdots\cdots \text{(Eq. 2.4.3)}$$

The Anstis mode is based on the assumption that the observed surface cracks and surface traces of sufficiently large radial cracks. By applying this mode, the K_{1c} of PK21, PK22 are 4.1 $Mpa\sqrt{m}$ and 5.33 $Mpa\sqrt{m}$ respectively.

Reported by Toshihiro lsobe et al [45], the Fracture Toughness was also can be estimated by indentation fracture method to evaluated Al203/Ni nanocomposite using the equation listed below:

$$K_{1c} = 0.026\frac{(EP)^{0.5}a}{c^{1.5}} \cdots\cdots \text{(Eq. 2.4.4)}$$

Where E is Young's Modulus, P is load allied for indentation, a is dimension and c is crack length measured from the center of the contact pattern. By applying this IF method, K_{1c} of PK21, PK22 is 5.41 $Mpa\sqrt{m}$ and 7.04 $Mpa\sqrt{m}$ respectively.

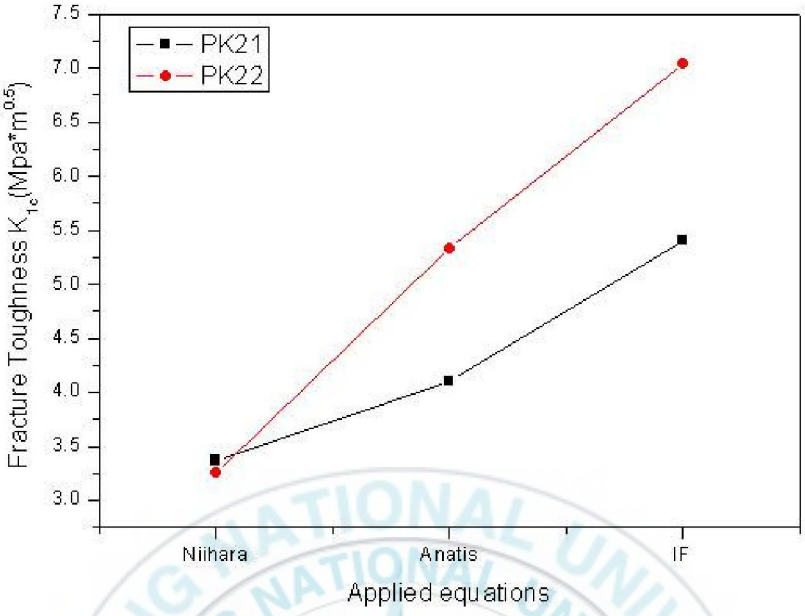

Fig. 32 Fracture Toughness of PK21, PK22 using various calculations

The results of the fracture toughness value using various calculations are list below as Fig. 32. All the results of PK21, PK22 showed a very brittle manner while PK22 is a little tougher than PK21, that may explain why PK22 insert showed shorter length missed in the cutting test while PK21 had longer, even with less Vickers hardness value than PK21, PK22 are likely to be more ductile to absorb crack propagation energy in the coating to prevent large fracture.

Ⅳ. Conclusion and Future Perspective

In this current investigation, we applied an advanced PVD method named PEMS to coat ceramic thin film coating TiSiCN on the WC-Co cutting insert to protect insert from wear, high friction, BUE and thermal un-stability, the PEMS utilizes a filament to generate plasma in order to serve as a source to provide

sputtering clean, conventional contamination was prevented in the coating since the magnetron did not start. High current, high deposition rate and high ion bombardment were achieved during the deposition due to the much more higher plasma density(25 times) than conventional magnetron sputtering, TMS was a good candidate to be served as a Si supply since it is less dangerous, easy to handle and do not corrode to the vacuum chamber, after deposition under different applying DC voltage, the properties of PK series ranged variously, coating thickness measured by SEM Cross-section Image was around 5um, the scratch test was introduced to study the adhesion properties, that the PK22 can have a largest critical load about 55N, while PK21 shows a lowest critical load about 20N, while tested in the XRD(X-ray diffraction Microscope), the spectrums revealed that the TiSiCN thin film consists of the crystalline structured Ti(C,N) with amorphous structure Si3N4 and amorphous carbon embedded in the matrix, the fracture toughness of the ceramic coating is improved by applying amorphous structure, the hardness is improved by applying C to replace N in TiN. Surface properties were characterized by AFM(Atomic Force Microscope), which indicated a fine surface. Then, cutting test was carried out at the median carbon steel in the CNC machining center, we used face milling at a severe cutting condition, the cutting tips were partly missed due to the high impact load, high rotation speed and high feed rate. The cutting force of PK21 shows the lowest cutting resistant force since we collected data from the very beginning of the test, the PK22 also shows a very low cutting force and surface roughness, very well anti-adhesion properties was observed at the PK series compared with the raw material since the existing of Ti in the coating. BUE is rarely seen due to the very good anti-adhesion properties. In the end, the WC-Co based PK21,PK21,PK22 were placed with another three specimens named PKSS20,PKSS21,PKSS22 based on the stainless steel under same coating condition, by applying Vickers Hardness Tester, the micro-hardness of the eight specimens(including two base material specimens), the indentation-induced fracture in the surface of six coated specimens were examined by applying different mode, the result shows that PK22

is a little tougher than PK21 and both are performing brittle properties, and this may be the reason why PK22 showed shorter missed length in the cutting test. So, in a word, with a high critical load, low surface roughness, relative low cutting resistant force and highest fracture toughness, PK22 is the most suitable candidate for dry enabled HSM.

However, since the attempt was carried out the first time, still some further work need to be considered in the future:

- Interlayer may be applied to examine the adhesion
- Critical cutting condition needs to be determined to get the optimum tool life and product quality.
- Harder cutting material needs to be applied
- Chemical composition needs to be studied.
- Fracture Toughness of TiSiCN coating needs to be improved.

Besides, TiSiCN ceramic hard thin film is not only served as cutting lubricant layer to protect cutting tools, as mentioned before, TiSiCN has a lot of applications such as erosion resistant coating, TBC in the high temperature, decoration…and also different deposition process which lead to various TiSiCN properties which must have a wider application, such as by applying plasma-enhanced technique, heavy bombardment technique, bias technique…and so on.

Ⅴ. Reference

1) Neil Canter, “Fabricating & Metalworking, the business of metal manufacturing”, July 13, 2008
2) G. Byrne, D. Dornfeld, B.Denkena, “Advanced Cutting Technology”
3) Http://www.endmill.com/pages/coatings.html
4) Patricia L. Smith, “The 10 commandments of dry high-speed machining**”,** 1998
5) Brian chapman, A wiley-interscience publication, JOHN WILEY & SONS, “Glow Discharge Processes: Sputtering and Plasma Etching”, Pages 235-285
6) Rointan F. Bunshah, “Handbook of deposition technologies for films and coatings”, Pages 70-91
7) Richard Fitzpatrick, Professor of Physics in The University of Texas at Austin, “The Physics of Plasmas”, Pages 124-154
8) Maissel and Glang, “Handbook of Thin film Technology”, McGraw-Hill, Inc, 1970, Pages 114-144
9) James A Brown, “Modern Manufacturing Process”, 1991, Pages 60~67
10) Nishad G. Deshpande, Jagdish C. Vyas, Ramphal Sharma, Thin Solid Films, Volume 516, Issue 23, 2008, Pages 8587-8593
11) Juergen M. Lackner, Wolfgang Waldhauser, Manfred Schwarz, Leonard Mahoney, Lukasz Major, Boguslaw Major, Vacuum, Vol. 83, Issue 2, 2008, Pages 302-307
12) Alicja Krella, Andrzej Czyżniewski, Wear, Vol. 265, Issue 7-8, 2008, Pages 963-970
13) J. Robertson, “Diamond-like amorphous carbon”, Pages 4-25
14) Ali Erdemir, et al, Appl.Phys, 2006, R311¨CR327 doi:10.1088/0022-3727/39/18/R01
15) S. Veprek, et al, Surface & Coating Technology, 2000, Pages 133-134
16) H.D Mannling, et al, Surface & Coating Technology, 2001, Pages 146-147.
17) Xiaodong Zhang, B.S., Beijing University of Aeronautics and Astronautics, 2003, “STRUCTURE AND MECHANICAL PROPERTIES OF Ti-Si-N COATINGS”
18) Ma SL, et al, Vac Sci Surface & Coating Technology, 2005, Pages143-148
19) Binnig, G.; Quate, C. F.; Gerber, Ch. Phys. Rev. Lett. 1986, Pages 56-58
20) S.L. Ma, D.Y. Ma, et al, Acta Mater , 2007, Pages 112-118

21) Shinya Imamura, et al, Surface & Coating Technology 202, 2007, Pages 820-825
22) Yan Guo, Shengli Ma, et al, Surface & Coating technology, 2007, Pages 5240-5243
23) Ali Erdemir, Christophe Donnet, J. Phys. D: Appl. Phys. 2006, Pages 311–327
24) Jun-Ha Jeon, et al, Surface & Coating technology, 2004, Pages 415-419
25) Dayan Ma, et al, Thin Solid Film, 2006, Pages 438-444
26) Badzian A, Badzian T. Appl Phys Lett 1993, 62; 3432
27) Ronghua Wei, et al, Surface & Coating Tchnology, 2006, Pages 4453-4459
28) Arsen Narimanyan, Applied Mathematical Modelling, Vol. 33, Issue 1, 2009, Pages 176-197
29) J.P. Davim, C. Maranhão, Materials & Design, Vol. 30, Issue 1, 2009, Pages 160-165
30) R. Jalili Saffar, M.R. Razfar, O. Zarei, E. Ghassemieh, Simulation Modelling Practice and Theory, In Press, Corrected Proof, Available online 2 September 2008
31) Wenling Chen, Wei Li, Ning Liu, Haidong Yang, Journal of Materials Processing Technology, Vol. 197, Issues 1-3, 2008, Pages 36-42
32) Shinya Imamura, et al, Surface & Coating Technology 202, 2007, Pages 820~825
33) A.Devillez, et al, Wear, 2007, Pages 931-942
34) John B. Wachtman and Richard A. Haber, “ceramic films and coatings”, Pages 28~33
35) Janusz NOWOTNY, “Science of ceramic interfaces”, Page 137-138
36) K.S. Woon, et al, Journal of Materials Processing Technology Vol. 195, Issues 1-3, 2008, Pages 204-211
37) H. Xu, et al, Surface & Coating Technology, 201, 2006, Pages 4236~4241
38) L. Ning , S.C. Veldhuis , K. Yamamoto, International Journal of Machine Tools & Manufacture, 2008, Pages 656~665
39) Roberto Dal Maschio, et al, Engineering Fracture Mechanics, Vol. 51, No.2, 1995, Pages 209~215
40) Yan Guo, et al, Material Research Society, Vol. 23, No. 9, 2008, Pages 2420~2427
41) Janghong Gong, Journal of the European Ceramic Society, 19, 1999, Pages 1585~1592

42) Janghong Gong, et al, Material Letters, 49, 2001, Pages 180~184
43) K.Niihara, Material Science Letters 2, 1983, Pages 221~223
44) S.Haussuhl, Z.Kristallogr. 120, 401, 1964
45) Toshihiro lsobe, et al, Ceramics International, Vol.34, Issue 1, 2008, Pages 213~217

Acknowledgement

It is such a flashing time that I passed the two-years' study like a dream, in the Surface modification Lab. where I struggled, confused, delighted and enjoyed, those are all my best memories among my career, I will never forget this delightful time spend here in PKUN.

I would like to thank my father Liu Yong and my mother Wang Fen who gave me financial support that I can keep my education going on, without their support which is not only money spending but also careful concern all the time. I'd like to thank my advisor, Prof. Kyu-Yong Lee who opened a new window for me and led to the area of thin film technology, although sometimes there is arguing in the study. I did my thesis work under his supervision, and he gave me lots of valued suggestions and also some financial support. I want to gave my best wished to him and wish me health and delight.

I would like to thank Prof. Yoon and Prof. Kim who gave me advices about my thesis and help modify it time and time again. Thank Prof. Yoon who gave me suggestions on the part of dry machining as the chairman of the committee, thank Prof. Kim who supplied me Vickers Hardness Tester and theories on the fracture mechanics that I can carry on my continuous work. Thank my lab mates Dae Hong, Tae Guan and Ei Dem who gave me lots of help for my living and language.